ISSN 1023-9855

Thoracic Medicine

Volume 41 • Number 2 • June 2026

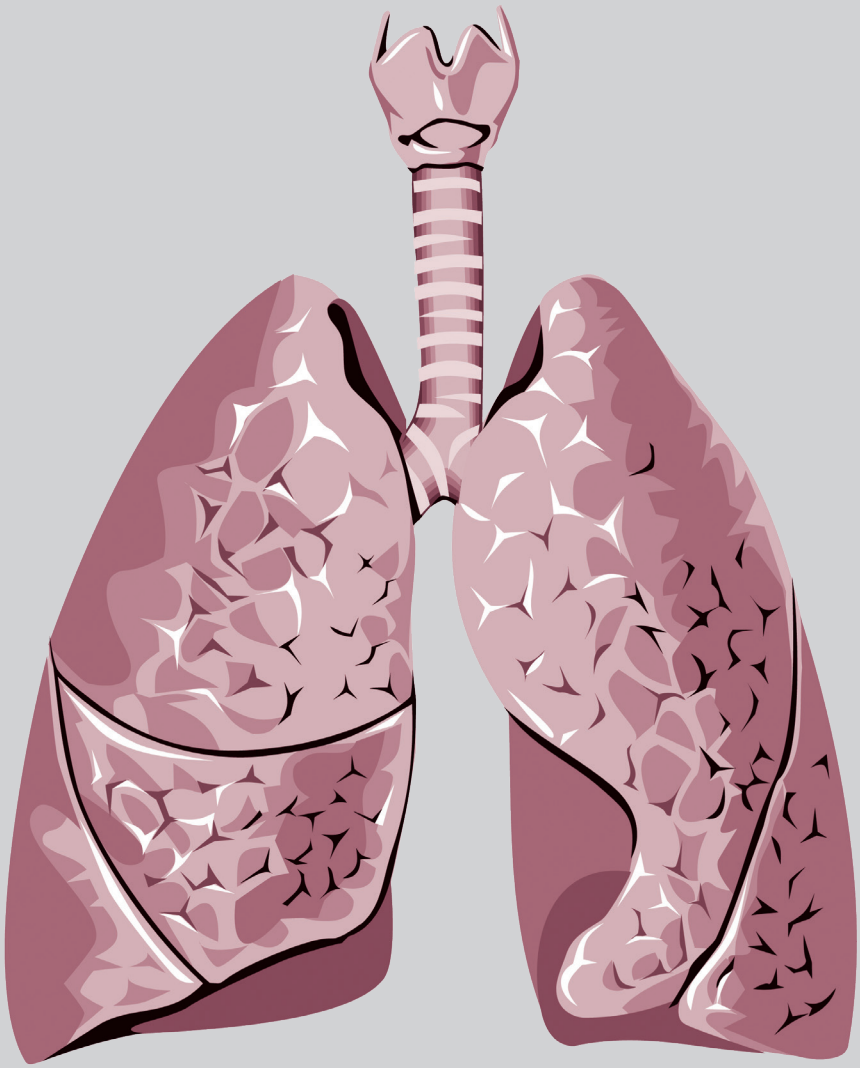

The Official Journal of

Taiwan Society of Pulmonary and Critical Care Medicine

Taiwan Society of Sleep Medicine

Taiwan Society for Respiratory Therapy

Taiwan Society of Tuberculosis and Lung Diseases

Thoracic Medicine

The Official Journal of
Taiwan Society of Pulmonary and Critical Care Medicine
Taiwan Society for Respiratory Therapy
Taiwan Society of Sleep Medicine
Taiwan Society of Tuberculosis and Lung Diseases

Thoracic Medicine

The Official Journal of
Taiwan Society of Pulmonary and Critical Care Medicine
Taiwan Society for Respiratory Therapy
Taiwan Society of Sleep Medicine
Taiwan Society of Tuberculosis and Lung Diseases

Volume 41
Number 2
June 2026

CONTENTS

Original Articles

Case Reports

Prognostic Implications of Pneumococcal Urine Antigen Positivity in Critically Ill COVID-19 Patients

Hsieh-Ping-Ju[1], Wei-An Chang[1,2], Ming-Ju Tsai[1,2], Chau-Chyun Sheu[1,2], Jen-Yu Hung[1,2], Cheng-Hao Chuang[1]

Background: *Streptococcus pneumoniae* is a major cause of pneumonia and has contributed to high mortality in respiratory infections. The impact of pneumococcal co-infection during the COVID-19 pandemic is unclear. This study evaluated the clinical effects of pneumococcal co-infection, as indicated by a positive urine antigen test (UAT), in severe COVID-19 patients admitted to a quarantine intensive care unit (ICU) in Taiwan.

Methods: From May to July 2022, 162 patients with severe COVID-19 were admitted to the COVID-19 quarantine ICU; 101 (62%) of the patients had available pneumococcal UAT results and detailed clinical data. These patients were divided into UAT-positive and UAT-negative groups to assess the impact of pneumococcal co-infection. Clinical characteristics, comorbidities, vaccination status, procalcitonin levels, and the use of advanced respiratory support were compared between the 2 groups.

Results: Pneumococcal antigen positivity was 18% (18/101). UAT-positive patients were older and had significantly higher APACHE-II scores (21.5 vs. 15, $p = 0.02$) and baseline procalcitonin levels (3.28 vs. 0.30 ng/mL, $p < 0.01$). The UAT-positive population received more empiric antibiotics (100% vs. 80%, $p = 0.04$) and required more advanced respiratory support (78% vs. 49%, $p = 0.036$). However, no significant differences were observed in ICU stay, hospital stay, or in-hospital mortality between the 2 groups. Prior pneumococcal vaccination did not significantly reduce mortality or disease severity.

Conclusion: Pneumococcal co-infection in severe COVID-19 patients was associated with increased disease severity and advanced respiratory support needs but not with higher mortality or prolonged hospitalization. Further research on the role of pneumococcal vaccination in COVID-19 outcomes is needed. ***(Thorac Med 2026; 41: 48-56)***

Key words: pneumococcal infection, pneumococcus urine antigen, COVID-19, respiratory failure

[1]Division of Pulmonary and Critical Care Medicine, Kaohsiung Medical University Hospital. [2]School of Medicine, College of Medicine, Kaohsiung Medical University, Kaohsiung, Taiwan.
Address reprint requests to: Dr. Cheng-Hao Chuang, Division of Pulmonary and Critical Care Medicine, Department of Internal Medicine, Kaohsiung Medical University Hospital, Kaohsiung Medical University No.100, Tzyou 1st Road, Kaohsiung 807, Taiwan.

Introduction

The COVID-19 disease was first reported in December 2019 in Wuhan, China. In March 2020, the World Health Organization (WHO) declared the novel coronavirus (COVID-19) outbreak a global pandemic.

Bacterial coinfection in COVID-19 patients was lower than in previous influenza pandemics [1]. However, bacterial coinfection was more frequently observed in intensive care unit (ICU) patients (14%) than in hospitalized patients (7%) [2]. Previous retrospective cohort studies have shown that bacterial coinfection increases the risk of ICU admission, mechanical ventilation (MV) use, and in-hospital mortality [3]. The most common bacterial pathogen associated with coinfection during COVID-19 was *Streptococcus pneumoniae* (*S. pneumoniae*) in cases with community-acquired pneumonia (CAP) [4-5].

S. pneumoniae is the leading cause of CAP worldwide and has been responsible for the highest proportion of mortality due to lower respiratory tract infections across all age groups from 1990 to 2019. A similar trend was observed during the COVID-19 era, despite the implementation of non-pharmaceutical interventions such as face mask use and mobility restrictions [6].

Microbiological evidence is the cornerstone of infectious disease management. However, the poor overall yield and quality of sputum samples have limited their clinical utility and impact on patient outcomes. Similarly, blood cultures have shown a low detection rate in non-severe CAP. The 2019 IDSA/ATS guidelines weakly recommend pneumococcal urine antigen testing (UAT) for severely ill patients [7].

The diagnostic performance of pneumococcal UAT has been reported as follows: sensitivity 78.57%, specificity 100%, positive predictive value 100%, negative predictive value 98.88%, and overall accuracy 90%. These metrics are comparable to sputum culture results but provide a more time-efficient approach to guide antibiotic therapy [8].

In a retrospective cohort study in Sweden, a positive pneumococcal UAT was associated with decreased use of broad-spectrum β-lactam monotherapy (OR 0.39, 95% CI 0.25–0.60) and reduced atypical pathogen coverage (OR 0.25, 95% CI 0.16–0.37), primarily in non-severe CAP cases [9]. However, in a prospective Italian study (SMACORE) involving 469 patients between October and December 2020, a positive pneumococcal UAT result was not associated with improvements in 30-day in-hospital mortality or ICU admission rates [10].

The prognosis of pneumococcal pneumonia in the context of COVID-19 coinfection remains unclear. In COVID-19 patients tested using UAT, *S. pneumoniae* infection was detected in 11.0% of individuals and was more common in severe cases than in moderate ones [11]. During the COVID-19 pandemic, non-invasive parameters for assessing disease progression became critical for predicting clinical outcomes. In our daily practice at a quarantine ICU in Taiwan (May–July 2022), we observed an increased detection rate of pneumococcal antigen in urine samples. The impact of bacterial coinfection indicated by a positive pneumococcal antigen test in critical COVID-19 patients is uncertain. Therefore, this study aimed to evaluate the prognostic value of pneumococcal infection and UAT use in patients with severe COVID-19 requiring ICU admission.

Methods

Study design

This single-center retrospective study was conducted from May to July 2022 at Kaohsiung Medical University Hospital, a major medical center in southern Taiwan. The study aimed to evaluate prognostic factors in patients with severe COVID-19 who were admitted to the quarantine ICU during the study period.

Electronic medical records were reviewed to collect data on baseline characteristics, comorbidities, disease severity, laboratory test results, pneumococcal UAT results upon ICU admission, blood and sputum culture findings, pneumococcal vaccination history, and clinical outcomes. The assessed clinical outcomes included the use of non-invasive and invasive ventilation, length of ICU and hospital stay, and mortality rate.

This study was conducted in accordance with the Declaration of Helsinki and was approved by the Institutional Review Board of Kaohsiung Medical University Hospital (KMUHIRB-E(I)-20250062). Written informed consent was not required.

Patients

Patients diagnosed with severe acute respiratory syndrome coronavirus 2 (SARS-CoV-2) who required quarantine ICU admission during the Omicron wave (May–July 2022) at our institution were enrolled in this study. A positive SARS-CoV-2 rapid antigen test or polymerase chain reaction (PCR) test was required for inclusion. Patients were excluded if they had end-stage renal disease, lacked pneumococcal UAT results upon admission, or were admitted to the surgical ICU without severe COVID-19 infection.

Definition of Outcomes

The duration of admission was calculated from the date of ICU admission to the date of ICU discharge or hospital discharge. Advanced respiratory support was defined as the use of a high-flow nasal cannula (HFNC) or invasive MV. Non-invasive ventilation with a bilevel positive airway pressure (BIPAP) machine was not available as an oxygen therapy option during the study period due to concerns about aerosol transmission.

In-hospital mortality was the primary outcome and was defined as death occurring during hospitalization, as post-discharge survival data were unavailable for a portion of the study population.

Statistics

Continuous variables were expressed as means and ranges, while categorical variables were reported as frequencies and percentages. Differences in baseline characteristics were analyzed using the unpaired Student's t-test for continuous variables and the Pearson chi-square test or Fisher's exact test for categorical variables. All statistical analyses were performed using GraphPad Prism version 9.5.1, with a p-value < 0.05 considered statistically significant.

Results

A total of 162 patients with severe COVID-19 who were admitted to the COVID-19 quarantine ICU during the study period were identified. Of these, 101 patients (62%) with available pneumococcal UAT results and detailed clinical information were included in the analysis. Patients were stratified into pneumococcal UAT-positive and UAT-negative groups to evaluate the clinical impact of superimposed

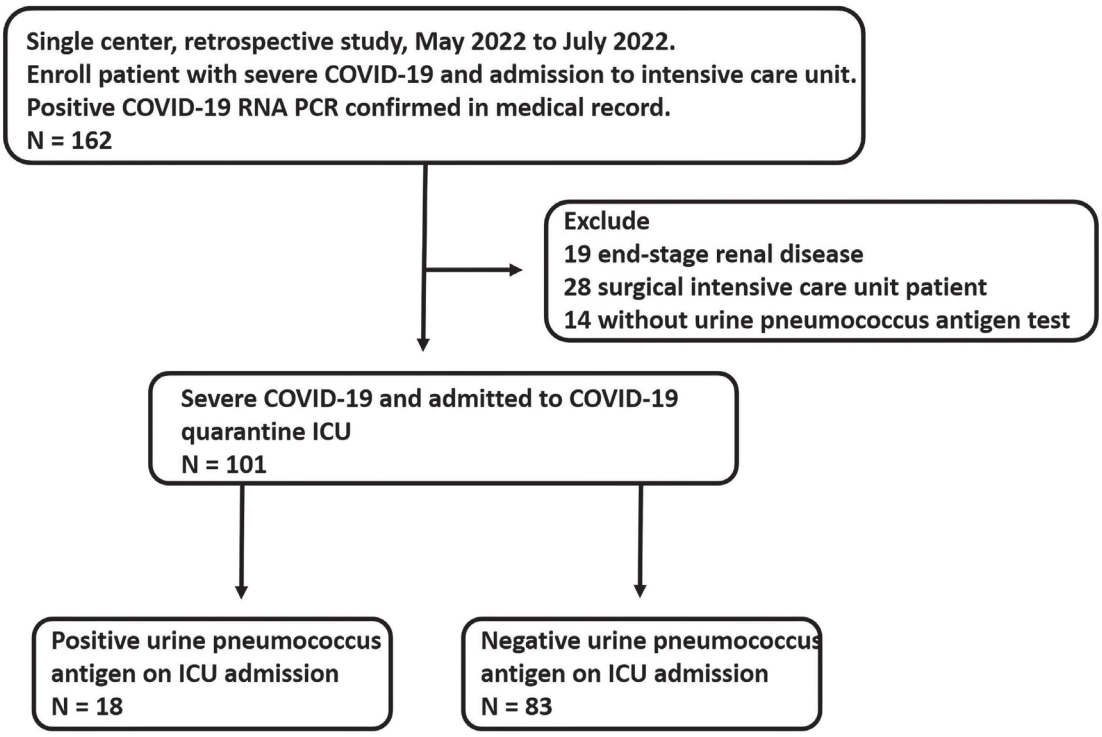

Fig. 1. Flow-chart of patient selection

pneumococcal infection in severe COVID-19.

The incidence of urine pneumococcal antigen positivity was 18% (18/101). The patient flowchart is presented in Figure 1, and baseline characteristics of the study population are summarized in Table 1. In the UAT-positive group, the median age was 80.5 years, with a predominance of female patients. Comorbidities and pneumococcal vaccination status were similar between the 2 groups. The majority of patients (75.2%) had not received either pneumococcal conjugate vaccine 13 (PCV13) or pneumococcal polysaccharide vaccine 23 (PPSV23), while 20.8% had received PPSV23.

The UAT-positive group had a significantly higher APACHE-II score than the UAT-negative group (21.5 vs. 15.0, $p = 0.02$). Additionally, procalcitonin (PCT) levels were significantly higher in the UAT-positive group (3.28 vs. 0.30 ng/mL, $p < 0.01$). A positive pneumococcal UAT was significantly associated with the use of empirical antibiotics ($p = 0.04$), with 100% of UAT-positive patients receiving antibiotics compared to 80% in the UAT-negative group. No culture-confirmed pneumococcal infections were identified in this cohort.

Patients with a positive pneumococcal UAT had a higher risk of requiring advanced respiratory support, including HFNC and MV (78% vs. 49%, $p = 0.036$). Although the duration of HFNC and MV use was numerically higher in the UAT-positive group, the difference did not reach statistical significance ($p = 0.76$). A positive pneumococcal UAT was not associated

Table 1. Baseline Characteristics of the Study Population.

	Pneumococcus UAT-negative N = 83	**Pneumococcus UAT-positive N = 18**	***P value***
Median age, y (range)	69 (27 -96)	80.5 (56 - 91)	p= 0.02
Gender, n (%)			p= 0.01
Male	59 (71%)	7 (39%)	
Female	24 (29%)	11 (61%)	
Comorbidity, n (%)			
Diabetes mellitus	30 (36%)	7 (39%)	p= 0.9
Chronic kidney disease	18 (27%)	4 (22%)	p= 0.9
APACHE-II scores, median (range)	15 (4-35)	21.5 (5-35)	p= 0.02
Positive *Streptoccocus pneumoniae* culture, n (%)	0 (0%)	0 (0%)	p> 0.99
Baseline PCT, Median, ng/mL (range)	0.30 (0.02-20.24)	3.28 (0.06-63.48)	p< 0.01
Empiric antibiotic use	66 (80%)	18 (100%)	p= 0.04
Previous pneumococcus vaccination, n (%)	21 (25%)	4 (22%)	p= 0.9
PCV13	3 (4%)	0 (0%)	
PPV23	17 (20%)	4(22%)	
Both	1(1%)	0 (0%)	

Acronyms:
UAT = urine antigen test
APACHE = Acute Physiology and Chronic Health Evaluation

with ICU length of stay (p = 0.65), hospital length of stay (p = 0.34) or increased in-hospital mortality (39% vs. 35%, p = 0.79) (Table 2). Furthermore, the risk of COVID-19-associated pulmonary aspergillosis (CAPA) did not significantly differ between groups (p = 0.9), likely due to its extremely low incidence.

There was no significant association between pneumococcal vaccination status and UAT positivity (p = 0.9). In addition, pneumococcal vaccination did not significantly reduce in-hospital mortality (40.0% in the vaccinated group vs. 34.2% in the non-vaccinated group, p = 0.64), advanced respiratory support duration (mean 7.9 days in the vaccinated group vs. 8.2 days in the non-vaccinated group, p = 0.93), urine pneumococcal antigen positivity rate (16.0% in the vaccinated group vs. 18.4% in the non-vaccinated group, p = 0.99), or disease severity as measured by APACHE-II scores (19.5 in the vaccinated group vs. 18.5 in the non-vaccinated group, p = 0.51) (Table 3).

Table 2. Clinical Outcomes of the Study Population.

	Pneumococcus UAT-negative N = 83	**Pneumococcus UAT-positive N = 18**	***P value***
ICU length of stay, days (range)	5 (1-77)	6.5 (1-26)	*p*= 0.65
Hospital length of stay, days (range)	15 (1-110)	15 (1-42)	*p*= 0.34
Advanced respiratory support, n (%)	41 (49%)	14 (78%)	*p*= 0.036
HFNC	16 (19%)	6 (33%)	*p*= 0.21
Invasive mechanical ventilation	30 (36%)	10 (56%)	*p*= 0.18
Mean duration of advanced respiratory support, days (range)	7.8 (0-71)	9.5 (0-60)	*p*= 0.63
HFNC	1.4 (0-20)	2.1 (0-16)	*p*= 0.53
Invasive mechanical ventilation	6.4 (0-71)	7.4 (0-60)	*p*= 0.76
Positivity of follow-up serum galactomannan	1 (1.2%)	0 (0%)	*p*= 0.9
In-hospital mortality	29 (35%)	7 (39%)	*p*= 0.79

Acronyms:
UAT = urine antigen test
HFNC = high-flow nasal cannula

Table 3. Efficacy of Pneumococcal Vaccination in Clinical Outcomes of the Study Population.

	Vaccinated N = 25	**Unvaccinated N = 76**	***P value***
Urine pneumococcus antigen positivity	16.00%	18.40%	*p*> 0.99
Mean APACHE-II score	19.5	18.5	*p*= 0.51
Advanced respiratory support	52%	56.76%	*p*= 0.82
Mean duration of advanced respiratory support, days (range)	7.9 (0-71)	8.2 (0-60)	*p*= 0.93
In-hospital mortality	40%	34.21%	*p*= 0.64

Acronyms:
APACHE = Acute Physiology and Chronic Health Evaluation

Discussion

In our study, the incidence of urine pneumococcal antigen positivity in COVID-19 patients was 18%, which is higher than in previous studies: 12% in the United States, 9% in Spain, and 13% in Italy [12, 13, 14]. This higher incidence may be attributed to the relatively greater disease severity and older age of patients in our study population.

In a pre-COVID-19 era study, pneumococcal UAT was positive in 12.8% of patients diagnosed with CAP. The baseline characteristics of that study population included a median age of 64.2 years, with male patients at 47.2%, and 41.7% having been admitted to the ICU within 72 hours of diagnosis. Those admitted to the ICU had a higher proportion of positive UAT results compared to those admitted to the general ward (15% vs. 8.8%, respectively; $p < 0.01$) [12].

In Barcelona, COVID-19 patients with pneumococcal pneumonia co-infection were predominantly female (57%), compared to those with negative pneumococcal testing (34%, $p < 0.001$). The median age of these patients was 68 years, and the 30-day mortality rate was 17% [13]. In the northern Italy COVID-19 pandemic, pneumococcal co-infection was observed in 13% of patients. The median age was 62.9 years, with a male-to-female ratio of 1:1. The in-hospital mortality rate was 15.4% [14].

In our ICU population, empirical antibiotic treatment was administered to all urine pneumococcal antigen-positive (UAg+) patients. No significant difference in mortality was observed between the UAg+ and UAg- groups, likely due to the fact that 80% of all patients received empirical antibiotics during hospitalization.

Pneumococcal UAT positivity was associated with higher APACHE-II scores and an increased need for respiratory support, including both invasive and non-invasive MV; however, it was not associated with an increased mortality rate. This may be attributable to the widespread use of empirical antibiotics and the comprehensive care system in place.

Among pneumococcal-vaccinated patients in our population, no significant reduction in risk (in terms of disease severity, advanced respiratory support, or death) was observed. This may be explained by several factors. First, the predominant serotypes of pneumococcal pneumonia could have shifted during the COVID-19 pandemic. A previous prospective study in Taiwan showed that the incidence of vaccine-type pneumococcal pneumonia declined between 2015 and 2018 in the adult population, particularly serotypes 19F and 6B. In contrast, the 3 most common non-PCV13 serotypes were 15A (15.2%), 23A (10.8%), and 15B/C (8.0%), which are not covered by either PCV13 or PPSV23 [15)].

Second, only 25% of patients had received at least 1 dose of either PCV13 or PPSV23. Although Taiwan has a robust health policy regarding pneumococcal vaccination compared to other countries, increased uptake of pneumococcal vaccination (primarily self-paid PCV13) has been observed in the post-COVID-19 era [16-17].

The incidence of CAPA was lower in our study population (1/101), which was significantly lower than the 17.5% reported in a 2024 meta-analysis [18]. This discrepancy may be related to differences in disease evolution and diagnostic efficacy. The incidence of CAPA increased by 50% during the vaccination era in ICU settings, with most patients undergoing bronchoalveolar lavage sampling [19].

Our study has several limitations. First, it was a retrospective, single-center study conducted over a relatively short period of time. Second, we did not validate the pneumococcal serotypes using the pneumococcal urine antigen test at our hospital. The urine pneumococcal antigen test used at Kaohsiung Medical University Hospital was the Binax NOW® test, which detects the c-polysaccharide antigen of S. pneumoniae. As a result, we could not differentiate the serotypes of pneumococcus during the COVID-19 pandemic, limiting our ability to accurately evaluate the effectiveness of vaccination. Future studies should consider using the Luminex urine pneumococcal test for more detailed analysis. Third, the possibility of false positives in pneumococcal UAT should be considered. False positives have been reported in individuals who are carriers of S. pneumoniae, those with a history of prior pneumococcal vaccination, patients infected with other Streptococcus species, and individuals with recurrent episodes of pneumococcal pneumonia [20].

The urine pneumococcal antigen test showed a positive correlation with disease severity and respiratory failure in severe COVID-19 patients. However, mortality was not significantly impacted, likely due to the high-quality healthcare system in place. The effect of pneumococcal vaccination on improving clinical outcomes was limited. Further research on vaccination strategies is needed to address secondary bacterial infections following viral infections and to enhance survival benefits.

Conclusion

The pneumococcal urine antigen test may offer prognostic value in critically ill COVID-19 patients requiring ICU admission. A positive test result upon admission was associated with elevated procalcitonin levels, higher APACHE II scores, and an increased need for advanced oxygen therapy, including HFNC and MV. However, prior pneumococcal vaccination did not lead to a reduction in mortality,MV duration, or disease severity in this cohort.

Acknowledgments

This study was supported by grants from Cardinal Tien Hospital (CTH112A2217).

References

1. Adler H, Ball R, Fisher M, *et al*. Low rate of bacterial co-infection in patients with COVID-19. Lancet Microbe 2020; 1: e62.
2. Lansbury L, Lim B, Baskaran V, *et al*. Co-infections in people with COVID-19: a systematic review and meta-analysis. J Infect 2020; 81: 266-275.
3. Patton MJ, Orihuela CJ, Harrod KS, *et al*. COVID-19 bacteremic co-infection is a major risk factor for mortality, ICU admission, and mechanical ventilation. Crit Care 2023; 27:34.
4. Garcia-Vidal C, Sanjuan G, Moreno-Garcia E, *et al*. Incidence of co-infections and superinfections in hospitalized patients with COVID-19: a retrospective cohort study. Clin Microbiol Infect 2021; 27: 83-88.
5. Moreno-Garcia E, Puerta-Alcalde P, Letona L, *et al*. Bacterial co-infection at hospital admission in patients with COVID-19. Int J Infect Dis 2022; 118: 197-202.
6. Infections GBDLR, Antimicrobial Resistance Collaborators. Global, regional, and national incidence and mortality burden of non-COVID-19 lower respiratory infections and aetiologies, 1990-2021: a systematic analysis from the Global Burden of Disease Study 2021. Lancet Infect Dis 2024; 24: 974-1002.
7. Metlay JP, Waterer GW, Long AC, *et al*. Diagnosis and treatment of adults with community-acquired pneumonia. An official clinical practice guideline of the American Thoracic Society and Infectious Diseases Society of America. Am J Respir Crit Care Med 2019; 200: e45-e67.

8. Khaleel M, Samreen S, Sirangi S, *et al*. Evaluation of a rapid urine antigen detection assay as a point-of-care test in the diagnosis of community-acquired pneumonia. Cureus 2023; 15: e44078.
9. Athlin S, Magnuson A, Spindler C, *et al*. Pneumococcal urinary antigen testing for antimicrobial guidance in community-acquired pneumonia-A register-based cohort study. J Infect 2022; 85,2: 167-173.
10. Valsecchi P, Colaneri M, Zuccaro V, *et al*. Impact of pneumococcal urinary antigen testing in COVID-19 patients: outcomes from the San Matteo COVID-19 Registry (SMACORE). J Pers Med 2021; 11.
11. Stahlfeld A, Glick LR, Ott IM, *et al*. Detection of pneumococcus during hospitalization for SARS-CoV-2. FEMS Microbes 2022; 3: xtac026.
12. West DM, McCauley LM, Sorensen JS, *et al*. Pneumococcal urinary antigen test use in diagnosis and treatment of pneumonia in seven Utah hospitals. ERJ Open Res 2016; 2.
13. Anton-Vazquez V, Cliville R. Streptococcus pneumoniae coinfection in hospitalised patients with COVID-19. Eur J Clin Microbiol Infect Dis 2021; 40: 1353-1355.
14. Desai A, Santonocito OG, Caltagirone G, *et al*. Effectiveness of Streptococcus pneumoniae urinary antigen testing in decreasing mortality of COVID-19 co-infected patients: a clinical investigation. Medicina (Kaunas) 2020; 56.
15. Chen CH, Janapatla RP, Su LH, *et al*. Incidence rates, emerging serotypes and genotypes, and antimicrobial susceptibility of pneumococcal disease in Taiwan: a multi-center clinical microbiological study after PCV13 implementation. J Infect 2022; 84: 788-794.
16. Fletcher MA, Vojicic J, Daigle D, *et al*. National recommendations for adult pneumococcal vaccination in countries of the WHO regions of Americas, Africa, Eastern Mediterranean, South East Asia, and Western Pacific. Vaccine 2024; 42: 126390.
17. Lan C, Chen YC, Chang YI, *et al*. Impact of COVID-19 outbreak on influenza and pneumococcal vaccination uptake: a multi-center retrospective study. Vaccines (Basel) 2023; 11.
18. Gioia F, Walti LN, Orchanian-Cheff A, *et al*. Risk factors for COVID-19-associated pulmonary aspergillosis: a systematic review and meta-analysis. Lancet Respir Med 2024; 12: 207-216.
19. Feys S, Lagrou K, Lauwers HM, *et al*. High burden of COVID-19-associated pulmonary aspergillosis in severely immunocompromised patients requiring mechanical ventilation. Clin Infect Dis 2024; 78: 361-370.
20. Grijalva CG, Wunderink RG, Zhu Y, *et al*. In-hospital pneumococcal polysaccharide vaccination is associated with detection of pneumococcal vaccine serotypes in adults hospitalized for community-acquired pneumonia. Open Forum Infect Dis 2015; 2: ofv135.

Clinicopathological and Prognostic Characteristics of Lymphoepithelial Carcinoma of the Lung: a Single-Institution Experience in Central Taiwan

Shao-En Hung[1], Yu-Ting Yu[2,3]

Introduction: According to the 2021 WHO classification, lymphoepithelial carcinoma of the lung (LCL) is an uncommon Epstein-Barr virus (EBV)-associated form of squamous cell carcinoma, predominantly affecting East Asian non-smokers. It shares morphological features with undifferentiated nasopharyngeal carcinoma (NPC) and has a favorable prognosis. This study retrospectively analyzed 16 LCL patients to evaluate clinical, pathological, and prognostic characteristics.

Methods: Patients diagnosed with LCL (January 2017– December 2024) at a medical center were included. Data on demographics, clinical stage (American Joint Committee on Cancer, 8th edition), treatments (surgery, chemotherapy, immunotherapy, radiotherapy), and pathology (immunohistochemistry, EBV-encoded small RNA in situ hybridization [EBER-ISH]) were collected. Statistical analyses included Fisher's exact test and Kaplan-Meier survival analysis using MedCalc version 23.

Results: Of the 4,726 patients with newly diagnosed lung cancer at our institution between 2017 and 2024, 16 (0.34%) were diagnosed with LCL. The median age of the patients at diagnosis was 58 years (range: 40–74), with a female predominance (56.3%) and 62.5% being non-smokers. Seven patients (43.8%) were asymptomatic at diagnosis, with lesions detected incidentally during health screening. Thirteen patients (81.3%) presented with advanced-stage disease (stage III/IV), which was significantly higher than in the non-LCL lung cancer group. Surgical resection was performed in 13 patients, with lobectomy being the most common procedure. Nine patients received combined chemotherapy and immunotherapy; however, most showed a poor response despite high PD-L1 expression in some cases. Six patients receiving immunotherapy (37.5%) experienced tumor recurrence, with a median time to recurrence of 15 months. The 2-year and 5-year overall survival rates were 100% and 57.1%, respectively.

Conclusion: LCL is a rare EBV-associated subtype of NSCLC with a predilection for Asian, non-smoking populations. Despite a generally more favorable prognosis than other

[1]Department of Emergency Medicine, Jen-Ai Hospital, Taichung, Taiwan. [2]Department of Pathology, School of Medicine, Chung Shan Medical University, Taichung, Taiwan. [3]Department of Pathology, Chung Shan Medical University Hospital, Taichung, Taiwan. [4]Department of Pathology, Li Gong Medical Clinic.
Address reprint requests to: Dr. Yu-Ting Yu, Department of Pathology, Li Gong Medical Clinic, Taichung, Taiwan 403, 7F., No. 16, Sec. 2, Taiwan Blvd., West Dist., Taichung City.

NSCLC subtypes, a high proportion of patients in this cohort presented with advanced-stage disease, and responses to immunotherapy were limited, even among those with high PD-L1 expression. These findings underscore the need for clinical awareness, timely diagnosis, and further studies to explore predictive biomarkers and optimize treatment strategies for this uncommon malignancy. ***(Thorac Med 2026; 41: 57-65)***

Key words: Lymphoepithelial carcinoma of the lung (LCL), lymphoepithelioma-like carcinoma (LELC), lung tumor, EBV virus

Introduction

Pulmonary lymphoepithelioma-like carcinoma (LELC) has been reclassified as lymphoepithelial carcinoma of the lung (LCL) and is now recognized as a variant of squamous cell carcinoma, according to the 2021 WHO classification [1]. This rare subtype of non-small cell lung carcinoma (NSCLC) predominantly affects East Asian non-smokers, and represents only 0.92% of all NSCLC cases [1-2]. A previous case series in Taiwan estimated that LCL accounts for just 0.9% of all lung cancers [2].

LCL is strongly associated with Epstein-Barr virus (EBV) infection and exhibits morphological features identical to those of undifferentiated nasopharyngeal carcinoma (NPC) [2-3]. Pathologically, it is characterized by a syncytial growth pattern of tumor cells with large vesicular nuclei, prominent nucleoli, and dense lymphocytic infiltration. Studies suggest that LCL is often diagnosed at an early stage and generally has a better prognosis than other NSCLC subtypes [4-8]

Existing literature on LCL remains limited to small retrospective series, most of which lack detailed clinicopathological correlation or long-term treatment outcomes. Furthermore, the biological behavior of LCL, particularly its response to modern therapeutic modalities such as immunotherapy, remains poorly understood [9-13]. As immune checkpoint inhibitors gain prominence in NSCLC treatment, the unclear significance of PD-L1 expression in EBV-associated tumors highlights the need for further clarification. The present study aims to address these gaps by providing a clinicopathological analysis of 16 patients diagnosed with LCL at a medical center in central Taiwan over an 8-year period. We compare the stage distribution of LCL with that of non-LCL NSCLC cases, assess patient demographics and clinical presentations, and evaluate the outcomes of various treatment strategies, including surgery, chemotherapy, and immunotherapy. Notably, our study investigates the discrepancy between high PD-L1 expression and limited immunotherapy response, a phenomenon that challenges current assumptions in the treatment of EBV-associated lung malignancies.

By expanding on the limited existing evidence, this study aims not only to improve the

clinical recognition and management of LCL but also to contribute novel insights into its pathogenesis and therapeutic responsiveness. Given the rarity of LCL and its distinct biological profile, we believe this study provides valuable data that may guide future diagnostic and therapeutic strategies, particularly in regions with high EBV prevalence.

Methods

Study population

This retrospective study included patients diagnosed with LCL between January 1, 2017, and December 31, 2024, at a medical center in central Taiwan. We searched the pathology report system using the keywords "lymphoepithelial carcinoma of the lung" or "lymphoepithelioma-like carcinoma" (the former term for lymphoepithelial carcinoma of the lung). The specimen type was not limited to surgical specimens, as biopsy specimens were also included.

Data collection and clinicopathological review

Data on patients' ethnicity, age, gender, smoking status, Eastern Cooperative Oncology Group (ECOG) performance status and clinical stage were collected. Tumor staging was determined based on the 8th edition of the American Joint Committee on Cancer (AJCC) staging system. Information regarding treatment modalities, including surgery, neoadjuvant chemotherapy, immunotherapy, and radiotherapy, was also recorded. Pathological findings, immunohistochemical stains, and the results of EBV-encoded small RNA in situ hybridization (EBER-ISH) were reviewed.

Statistical analysis

We conducted statistical analyses using MedCalc version 23, which included comparing stage distributions with Fisher's exact test and generating Kaplan-Meier survival curves with log-rank tests for survival analysis.

Results

Patient Demographics and Clinical Presentation

A total of 4726 new lung cancer cases were diagnosed at our institute during the study period; 16 (0.34%) of these cases were LCL. Adenocarcinoma and squamous cell carcinoma were the predominant histological subtypes, accounting for 86% and 6.9% of all lung cancer cases, respectively. All identified LCL patients were of Chinese ethnicity and had no prior history of NPC. Females constituted the majority of the LCL cohort (n=9, 56.3%) (Table 1). The median age at diagnosis for LCL patients was 58 years (range: 40–74 years), and the median follow-up duration was 34 months. With regard to smoking history, 10 patients (2.5%) were non-smokers, 5 were current smokers, and 1 was a former smoker; data on the specific pack-years of smoking were not available.

A significant portion of patients (43.8%) presented no symptoms, and their lesions were found incidentally during a health exam. Less common symptoms were cough, chest tightness, and finger clubbing.

In the LCL group (Fig. 1), 3 patients (18.8%) were diagnosed with stage I/II, 8 (50%) with stage III, and 5 (31.3%) with stage IV disease. Fisher's exact test revealed a significantly higher proportion of patients with stage III/IV disease compared to those with stage I/II (P = 0.0106). In the non-LCL lung cancer group, the distribution was as follows: stage I/II 55.3%, stage III 9.9%, and stage IV 34.7%. Fisher's

Table 1. Clinical Data of Patients with Lymphoepithelioma-like Carcinomas of the Lung.

Case No	Sex	Age	Smoking history	Clinical stage	ECOG	Treatment	Outcome
1	M	67	no	I	0	SG	alive,15 mo.
2	M	69	yes	I	1	SG, sCRT	alive, 54 mo.
3	F	71	no	II	0	SG, CT	recurrence, 10 mo.; alive, 45 mo.
4	F	40	no	III	0	SG, sCRT, IO	alive, 14 mo.
5	M	52	yes	III	1	NAC, SG, CT, IO	alive, 29 mo.
6	F	51	no	III	NA	NAC, SG, CT, IO	recurrence, 20 mo.; died, 38 mo.
7	F	59	no	III	1	SG, CT	alive,25 mo.
8	F	43	no	III	0	SG, sCRT, IO	recurrence, 8 mo.; alive, 12 mo.
9	M	74	yes	III	1	NAC, SG, CT	alive, 9 mo.
10	F	42	no	III	0	SG, CT, IO	recurrence, 28 mo.; died, 51 mo.
11	F	54	no	III	0	SG, CT, IO	recurrence, 2 mo.; alive, 70 mo.
12	M	67	yes	IV	1	SG, CT, IO	alive, 44 mo.
13	M	63	yes	IV	1	sCRT, IO	alive, 33 mo.
14	F	57	no	IV	0	NAC, SG, RT, IO	recurrence, 29 mo.; alive, 34 mo.
15	M	66	yes	IV	1	CT	alive, 13 mo.
16	F	53	no	IV	1	CT	alive, 34 mo.

SG: surgery; sCRT: sequential chemoradiotherapy; CT: chemotherapy;
I O: immunotherapy; NA: not available; RT: radiotherapy; NAC: neoadjuvant chemotherapy

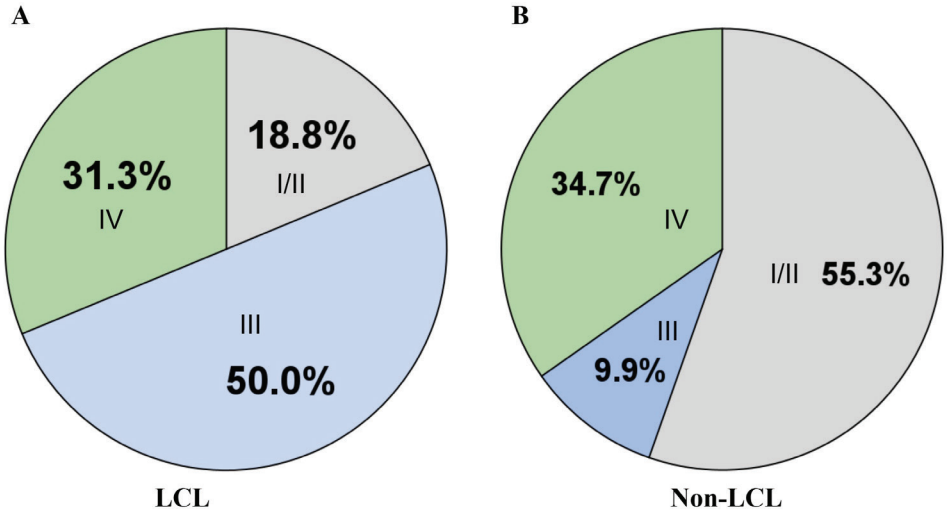

Fig. 1. Stage distribution of LCL and other non-LCL patients.
Note: Among the LCL group, 3 patients (18.8%) were diagnosed with stage I/II, 8 (50%) with stage III, and 5 (31.3%) with stage IV disease. In the non-LCL lung cancer group, the distribution was as follows: stage I/II: 55.3%, stage III: 9.9%, and stage IV: 34.7%

exact test also showed a statistically significant difference in stage distribution between the LCL and non-LCL groups ($P < 0.001$) (Fig. 1).

Treatment and Outcomes

Three patients were considered inoperable and only had a biopsy. For those patients who were able to undergo surgery, the type of surgery was based on the tumor's location and surgical findings. The surgeries performed included wedge resection for 1 patient, lobectomy for 11 patients, and pneumonectomy for 1 patient. Most patients received chemotherapy, except those with stage I disease (Table 1). Two patients, initially diagnosed as stage I/II, were later found to be stage III after surgery, based on the postoperative pathological reports.

The chemotherapy regimen was predominantly cisplatin-based, with adjustments made to the dosage and treatment plan based on the patient's age, clinical condition, and performance status. Nine patients in this study received both immunotherapy (either pembrolizumab or atezolizumab) and chemotherapy. Notably, 3 of these patients exhibited a PD-L1 expression level exceeding 50%. Despite this, all 3 of these patients experienced disease progression.

Tumor recurrence was observed in 6 patients. The sites of recurrence included the subcarinal lymph nodes (1 patient), supraclavicular lymph nodes (1 patient), abdominal lymph nodes (1 patient), neck (2 patients), ipsilateral lung (1 patient), adrenal gland (1 patient), and bilateral lungs (1 patient). The median time to recurrence was 15 months (range: 2–29 months).

Two patients died of the disease. Both of these patients had clinical stage III disease and experienced disease recurrence at 20 and 28 months, respectively (Table 1). Kaplan-Meier analysis indicated that 2- and 5-year overall survival (OS) rates were 100% and 57.1%, respectively (Fig. 2).

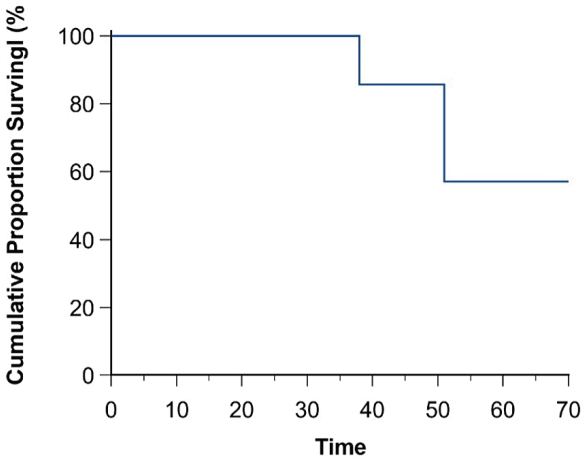

Fig. 2. Survival Curves for Patients with LCL.
Note: The overall survival rates for LCL at 2 and 5 years were 100% and 57.1%, respectively.

Pathology Findings

Histologically, tumor cells exhibited poorly defined cytoplasmic borders. Nuclei were round, oval, or elongated, displaying vesicular or finely granular chromatin and prominent eosinophilic nucleoli. A hallmark finding was the close association of neoplastic cells with a dense lymphoplasmacytic infiltrate, consistent with the diagnosis of LCL (Fig. 3). All specimens showed positive EBER-ISH, a diagnostic requirement for LCL as defined by the 2021 WHO classification of tumors. In a subset of cases, immunohistochemical analysis revealed positive staining for p40, p63, and cytokeratin, supporting the classification of LCL as a subtype of squamous cell carcinoma, as per the 2021 WHO guidelines [1, 6].

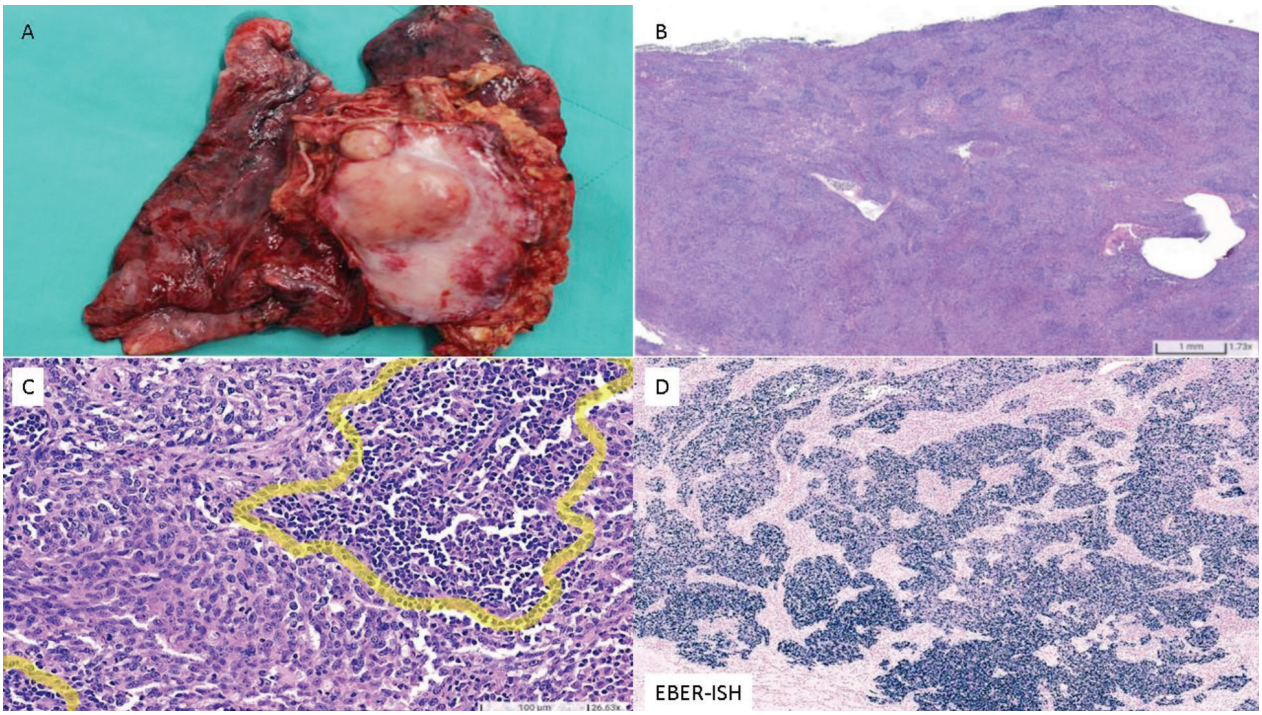

Fig. 3. Gross and Microscopic Findings.
Note: (3A) Gross findings of a lobectomy specimen. (3B) Low-power view of the tumor revealed a lymphocytic-rich stroma. (3C) The characteristic features of LCL, including abundant infiltrating lymphocytes (yellow circle), are evident. The tumor exhibited indistinct cell borders and prominent nucleoli. (3D) The tumor was EBER-ISH positive.

Discussion

This study provides a comprehensive analysis of 16 ethnic Chinese patients diagnosed with LCL, a rare subtype of NSCLC. The demographic and clinical characteristics of our cohort, along with the treatment outcomes and pathologic findings, offer valuable insights into the behavior and management of this uncommon malignancy.

All patients in our study were of Chinese ethnicity, with a slight female predominance (56.3%). This observation concurs with earlier reports demonstrating a female predominance. The demographic trend reflects the epidemiological profile of the disease, with most cases occurring in individuals from Asia, where EBV is widely endemic. Reports of cases in non-Asian populations, such as Caucasians, are exceptionally rare [1, 14-15]. The median age at diagnosis was 58 years, aligning with the typical age range reported in the literature for LCL [1].

Notably, 43.8% of patients in our cohort were asymptomatic, with lesions incidentally detected during routine health examinations. This finding is in line with previous reports, which have shown that many cases of LCL are incidentally identified in asymptomatic individuals [5, 8, 15-16]. Among those with advanced-

stage disease (stage III/IV, 81.3%), up to 38.5% were asymptomatic, further illustrating the diagnostic challenge in asymptomatic patients.

Although earlier studies have predominantly reported early-stage presentation [2, 6, 9, 11], our cohort demonstrated a significantly higher proportion of advanced-stage disease (P = 0.0106). This discrepancy underscores the difficulty in achieving early diagnosis and highlights the possible need for clinical surveillance, particularly among high-risk populations such as individuals from EBV-endemic regions and female patients.

Surgical resection remains the cornerstone of treatment for operable LCL, with lobectomy being the most frequently performed procedure in our cohort. However, 3 patients were deemed inoperable, reflecting the advanced stage at presentation in some cases. Adjuvant chemotherapy, primarily cisplatin-based regimens, was administered to most patients, except those with pathologic stage I disease. One patient with stage I disease underwent surgery alone and remained disease-free at the 15-month follow-up. The use of immunotherapy, specifically pembrolizumab or atezolizumab, in 9 patients represented a contemporary approach to managing advanced LCL. However, the response seemed suboptimal, with only 1 patient achieving a complete response at the 14-month follow-up, and another showing stable disease at 33 months. Recurrent disease was observed in 5 patients, with a median time to recurrence of 20 months (range, 6–29 months).

The lack of response in most patients, including the 3 with high PD-L1 expression (>50%), is intriguing. Indeed, most published studies suggest that higher PD-L1 expression is associated with a better response to immunotherapy. However, our cases did not follow this trend. One possible reason is the limited number of cases in both our study and in previous reports, as well as differences in disease stage and chemotherapy regimens. Recent studies have suggested that the co-expression of PD-L1 and LAG-3 may correlate with immunotherapy outcomes. Additionally, certain genes have been implicated in drug resistance. Further standardized investigations are necessary to elucidate these associations [9, 11-12].

The recurrence rate of 37.5% (6 patients in this cohort) and the median time to recurrence of 15 months highlight the aggressive nature of LCL and the need for close follow-up. The diverse sites of recurrence, including lymph nodes, lungs, and distant organs, emphasize the systemic nature of the disease and the importance of comprehensive surveillance strategies.

The 2- and 5-year OS rates for patients with LCL were 100% and 57.1%, respectively, suggesting that LCL may be associated with a more favorable prognosis than other NSCLC subtypes. In contrast, the 2- and 5-year OS rates for the overall NSCLC population at our institute were approximately 83% and 52%, respectively. This finding is consistent with previous studies reporting better outcomes in LCL patients. The 2 deaths in our cohort occurred in patients with stage III disease and recurrent disease, highlighting the poor prognosis associated with advanced-stage LCL and disease recurrence. However, log-rank test analysis did not reveal a statistically significant impact of recurrence on survival (P = 0.2649), which may be attributed to the limited sample size.

The histologic features observed in our cohort, including poorly defined cytoplasmic borders, vesicular chromatin, and prominent nucleoli, are characteristic of LCL. The close association of neoplastic cells with a dense lym-

phoplasmacytic infiltrate further supports the diagnosis. The universal positivity of EBER-ISH among our specimens confirmed the association of LCL with EBV infection, a hallmark feature, as per the 2021 WHO classification. The immunohistochemical positivity for p40, p63, and cytokeratin reinforces the classification of LCL as a subtype of squamous cell carcinoma, providing a clear pathologic framework for diagnosis.

This study has several limitations, including its small sample size and single-center design, which may limit the generalizability of the findings. Furthermore, the retrospective nature of the study introduces potential biases in data collection and analysis. The lack of long-term follow-up of some patients may also affect the accuracy of survival estimates.

Conclusion

In conclusion, LCL is a rare malignancy with a predilection for Asian populations. This study highlights the clinical challenges associated with LCL, particularly the frequent absence of symptoms at presentation and the high prevalence of patients diagnosed at advanced stages. In our cohort, responses to immunotherapy were generally limited, even among patients with high PD-L1 expression. Possible explanations for this observation have been discussed in detail within the article. In addition, the relatively high recurrence rate emphasizes the need for post-treatment surveillance. Although this study is limited by its retrospective design, small sample size, and single-center setting, it provides insights into the clinical and pathological characteristics of LCL in EBV-endemic regions. Further multi-center studies with larger cohorts and longer follow-up periods are warranted to better elucidate the disease course and to develop more effective strategies for diagnosis and treatment.

References

1. Chou, TY, Wong MP, Chang YL. Lymphoepithelial carcinoma of the lung. in WHO classification of tumours series (5th ed., Vol. 5). International Agency for Research on Cancer 2021, Lyon (France): International Agency for Research on Cancer
2. Carbone A, Micheau C. Pitfalls in microscopic diagnosis of undifferentiated carcinoma of nasopharyngeal type (lymphoepithelioma). Cancer 1982; 50(7): 1344-1351.
3. Bégin LR, Eskandari J, Joncas J, *et al*. Epstein-Barr virus related lymphoepithelioma-like carcinoma of lung. J Surg Oncol 1987; 36(4): 280-283.
4. Ho JC, Wong MP, Lam WK. Lymphoepithelioma-like carcinoma of the lung. Respirology 2006; 11(5): 539-545.
5. Han AJ, Xiong MF, Gu YY, *et al*. Lymphoepithelioma-like carcinoma of the lung with a better prognosis. A clinicopathologic study of 32 cases. Am J Clin Pathol 2001; 115: 841-850.
6. Jiang WY, Wang R, Pan XF, *et al*. Clinicopathological features and prognosis of primary pulmonary lymphoepithelioma-like carcinoma. J Thorac Dis 2016; 8(9): 2610-2616.
7. Sathirareuangchai S, Hirata K. Pulmonary lymphoepithelioma-like carcinoma. Arch Pathol Lab Med 2019; 143(8): 1027-1030.
8. Jiang WY, Wang R, Pan XF, *et al*. Clinicopathological features and prognosis of primary pulmonary lymphoepithelioma-like carcinoma. J Thorac Dis 2016; 8(9):2610-2616.
9. Fang W, Hong S, Chen N, *et al*. PD-L1 is remarkably over-expressed in EBV-associated pulmonary lymphoepithelioma-like carcinoma and related to poor disease-free survival. Oncotarget 2015; 6(32): 33019-33032.
10. Zhong YM, Yin K, Chen Y, *et al*. PD-1/PD-L1 combined with LAG3 is associated with clinical activity of immune checkpoint inhibitors in metastatic primary pulmonary lymphoepithelioma-like carcinoma. Front Immunol 2022; 13: 951817.
11. Zhou N, Tang H, Yu S, *et al*. Anti-PD-1 antibodies, a

novel treatment option for advanced chemoresistant pulmonary lymphoepithelioma carcinoma. Front Immunol 2022; 13: 1001414.
12. Liu Y, Long L, Liu J, *et al*. Case Report: Anlotinib reverses nivolumab resistance in advanced primary pulmonary lymphoepithelioma-like carcinoma with FGFR3 gene amplification. Front Oncol 2021; 11: 749682.
13. Sasaki A, Kato T, Ujiie H, *et al*. Primary pulmonary lymphoepithelioma-like carcinoma with positive expression of Epstein-Barr virus and PD-L1: a case report. Int J Surg Case Rep 2021; 79: 431-435.
14. Huang YC, Hsueh C, Ho SY, *et al*. Lymphoepithelioma-like carcinoma of the lung: an unusual case and literature review. Case Rep Pulmonol 2013; 143405.
15. Chang YL, Wu CT, Shih JY, *et al*. New aspects in clinicopathologic and oncogene studies of 23 pulmonary lymphoepithelioma-like carcinomas. Am J Surg Pathol 2002; 26(6): 715-723.
16. Tay CK, Chua YC, Takano A, *et al*. Primary pulmonary lymphoepithelioma-like carcinoma in Singapore. Ann Thoracic Med 2018; 13(1): 30-35.

Longitudinal Analysis of Type 2 Inflammatory Markers and Clinical Outcomes in T2-High Severe Asthma Patients Treated with Benralizumab

Chia-Wei Chang[1], Shin-Wei Wu[1], Ying-Chieh Chen[1], Li-Ting Cheng[1], Shin-En Tang[1,2,3], Chen-Liang Tsai[1], Chia-Hsin Liu[1]

Introduction: This study investigated the effects of benralizumab on dynamic changes in type 2 (T2) markers (blood eosinophils, total IgE levels) and their correlations with clinical outcomes in T2-high severe asthma.

Methods: Twenty patients with severe eosinophilic asthma treated with benralizumab were prospectively followed. Assessments included Asthma Control Test (ACT) scores, forced expiratory volume in 1 second (FEV1), acute exacerbations (AEs), oral corticosteroid (OCS) use, and T2 markers at baseline, 6 months, and 12 months.

Results: Benralizumab significantly improved ACT scores at 6 months (5.88 ± 1.49, p = 0.01) and 12 months (5.57 ± 1.74, p = 0.04), with FEV1 increasing by 0.33 ± 0.11 L at 6 months (p = 0.049) and 0.056 ± 0.01 L at 12 months (p = 0.010). AE frequency and OCS use significantly decreased, with AE reductions of 1.93 ± 0.35 (p = 0.0002) and 1.27 ± 0.29 (p = 0.0024), and OCS dose reductions of 4.53 ± 0.89 mg (p = 0.0003) and 5.00 ± 1.3 mg (p = 0.006) at 6 and 12 months, respectively. Blood eosinophils significantly decreased, while total IgE levels showed no significant changes. Baseline blood eosinophil and baseline total IgE levels showed a moderate correlation (r = 0.45, p = 0.041). Baseline total IgE levels were inversely correlated with OCS reductions at 6 months (r = -0.54, p = 0.038) and 12 months (r = -0.50, p = 0.049).

Conclusion: Benralizumab significantly improved clinical outcomes in T2-high severe asthma and influenced T2 marker dynamics, with baseline total IgE levels correlated with OCS dose reductions. ***(Thorac Med 2026; 41: 66-76)***

Key words: T2-high severe asthma, benralizumab, eosinophils, IgE

[1]Division of Pulmonary and Critical Care Medicine, Department of Internal Medicine, Tri-Service General Hospital, National Defense Medical Center, Taipei, Taiwan. [2]Institute of Aerospace and Undersea Medicine, National Defense Medical Center, Taipei, Taiwan. [3]Department of Medicine, Tri-Service General Hospital Songshan Branch, National Defense Medical Center, Taipei, Taiwan.

Address reprint requests to: Dr. Chia-Hsin Liu, Division of Pulmonary and Critical Care Medicine, Department of Internal Medicine, Tri-Service General Hospital, National Defense Medical Center, 325, Section 2, Cheng-Gung Road, Nei-Hu Dist. 114, Taipei, Taiwan.

Introduction

Severe asthma is defined as a subset of difficult-to-treat asthma that remains uncontrolled despite adherence to maximally optimized high-dose inhaled corticosteroid (ICS) and long-acting beta-agonist (LABA) therapy, along with the management of contributing factors [1]. Type 2 (T2) inflammation, the defining feature of T2-high severe asthma, is characterized by elevated blood eosinophil levels and increased fractional exhaled nitric oxide (FeNO), and is frequently associated with atopy and elevated serum total IgE levels [2-3]. These markers are widely used to assess disease severity and predict treatment responses. Recent progress in severe asthma treatment has included the development of targeted biological therapies, offering significant benefits, especially for patients with T2-high severe asthma [4].

Benralizumab, an anti-IL-5 receptor alpha monoclonal antibody, selectively depletes eosinophils via antibody-dependent cell-mediated cytotoxicity (ADCC) [5]. This biologic therapy effectively targets a key inflammatory pathway in T2-high severe asthma, leading to better asthma control, improved lung function, fewer exacerbations, and reduced reliance on oral corticosteroids (OCS) [6]. Furthermore, anti-IL-5/IL-5Rα biologics significantly reduced blood eosinophils, with benralizumab use demonstrating nearly complete depletion [7]. Higher blood eosinophil levels strongly predict a favorable response to benralizumab [8]. Nevertheless, the dynamic changes with T2 markers, including blood eosinophils and serum total IgE levels, during benralizumab treatment, and their relationship with clinical outcome improvements remains underexplored.

This study aims to evaluate the longitudinal effects of benralizumab on blood eosinophil levels and serum total IgE levels, and to examine how changes in these biomarkers are associated with clinical outcome improvements, including asthma control, lung function, exacerbation rates, and steroid use, over 12 months in patients with T2-high severe asthma. We hypothesized that blood eosinophils and total IgE levels would have distinct response patterns to benralizumab treatment, with their dynamic changes being associated with specific clinical improvements in patients with T2-high severe asthma.

Methods

Setting and participants

All adult patients who initiated benralizumab treatment between January 2021 and September 2023 at the tertiary asthma clinic of Tri-Service General Hospital, National Defense Medical Center, Taipei, Taiwan, were included in this study. The biological therapy was administered under Taiwan's National Health Insurance (NHI) system, which enforces a rigorous application process with specific eligibility criteria for each medication. For benralizumab, patients were required to have severe eosinophilic asthma (blood eosinophil count ≥300 cells/μL in the past year), persistent symptoms despite Step 5 therapy as outlined by the GINA guidelines, ongoing use of OCS (≥5 mg prednisolone daily or equivalent) for at least 6 months, and a history of at least 2 asthma exacerbations (AE) in the previous year, including 1 that required emergency care. Treatment continuation was assessed every 6 months, with eligibility contingent upon demonstrating objective improvements in FEV1, Asthma Control Test (ACT) scores, and exacerbation frequency, or oral steroid use. Monoclonal antibody

Table 1. Baseline Characteristics of the Study Population (n = 20).

Age (years)	52.9 ± 16.6
Sex (%)	
Man	40
Woman	60
BMI (kg/m2)	24.6 ± 4.6
Smoking state (%)	
Never-smoker	73.3
Former smoker	20
Current smoker	6.7
ACT score	14.8 ± 3.2
Pre-BD FEV1/FVC (%)	71.7 ± 16.1
Pre-BD FEV1(L)	1.94 ± 1.1
Pre-BD FEV1 (% predicted)	71.7 ± 16.0
Blood eosinophil counts (cells/μL)	376.5 ± 283.4
Blood total IgE levels (IU/mL)	499.7 ± 388.7
Exacerbations in the previous 6 months	2.3 ± 1.2
OCS (mg/day)	7.7 ± 4.6
Baseline inhalers	
ICS/LABA (%)	13.3
ICS/LABA/LAMA (%)	86.7

Data are presented as mean ± standard deviation.
Abbreviations: ACT, Asthma Control Test; BD, bronchodilator; BMI, body mass index; FEV1, forced expiratory volume in the first second; ICS, inhaled corticosteroid; LABA, long-acting bronchodilator; LAMA: long-acting muscarinic antagonist; OCS, oral corticosteroid.

injections were administered by trained nursing staff, prescriptions were managed through hospital pharmacies, and inhaler techniques were regularly reviewed to ensure proper usage.

Assessments

All patients underwent comprehensive assessments at baseline, and at 6 and 12 months, with data systematically recorded during each evaluation. Assessment interviews were conducted by trained respiratory medical and nursing staff. Collected data included patient demographics, asthma medication usage, ACT scores, lung function parameters, exacerbation history, blood eosinophil counts, serum total IgE levels, and maintenance OCS doses. Lung function tests were performed in accredited respiratory laboratories by trained technical staff using instruments calibrated on the day of testing. Predicted lung function values were derived from the Global Lung Initiative reference set [9]. All tests adhered to European Respiratory Society and American Thoracic Society guidelines [10], and bronchodilators were withheld on the day of testing, as per protocol. An exacerbation was defined as a worsening of asthma symptoms—

such as increased shortness of breath, wheezing, chest tightness, or cough—requiring changes in treatment, including increased reliever medication use, systemic corticosteroids, or emergency medical care [1]. Exacerbation frequency was determined based on the patient's report during interviews.

Statistical analysis

Continuous variables were reported as mean ± standard deviation (SD), and categorical variables were expressed as frequencies and percentages. Descriptive statistics were used to summarize patient demographics and clinical characteristics. Repeated measures ANOVA was employed to evaluate changes in continuous outcomes at baseline, 6 months, and 12 months, with post-hoc tests applied to account for multiple comparisons (*p <0.05, **p <0.01). Correlations between blood eosinophil counts and total IgE levels were analyzed using Pearson's correlation, with results reported as correlation coefficients (r) and corresponding p-values. To visualize associations, a correlation heatmap was constructed, highlighting significant relationships between clinical outcomes and T2 marker changes in patients receiving benralizumab. Statistical analyses were conducted using SPSS software (version 29).

Results

A total of 25 patients received benralizumab during the study period; however, 2 patients switched treatments, and 3 discontinued therapy before the 6-month outcome assessment. As a result, 20 patients who completed at least 6 months of treatment were included in the analysis (Fig. 1). The mean age of the benralizumab group was 52.9 ± 16.6 years, with 40% men

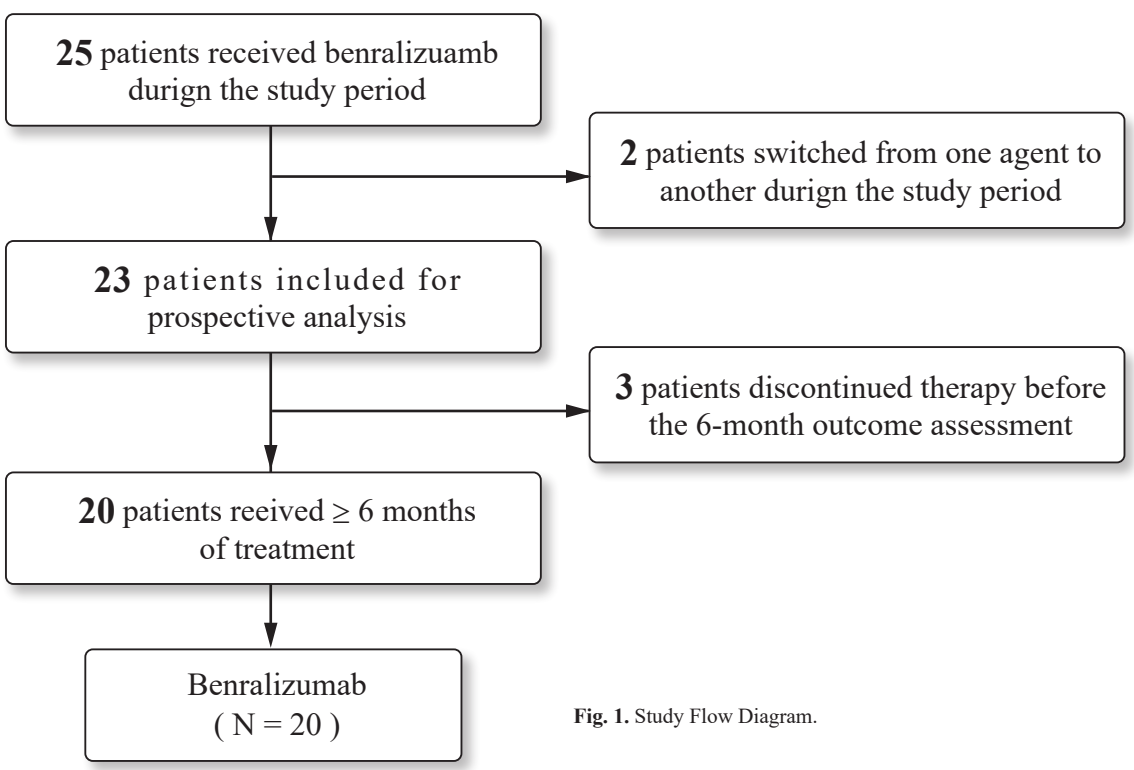

Fig. 1. Study Flow Diagram.

and 60% women. The average BMI was 24.6 ± 4.6 kg/m². Most patients were never-smokers (73.3%), with 20% being former smokers and 6.7% current smokers. Baseline lung function measurements showed a pre-bronchodilator FEV1 of 1.94 ± 1.1 L, corresponding to 71.7 ± 16.0% of the predicted value, and a FEV1/FVC ratio of 71.7 ± 16.1%. The baseline ACT score was 14.8 ± 3.2, indicating suboptimal asthma control. T2 inflammatory markers revealed a mean blood eosinophil count of 376.5 ± 283.4 cells/μL and a mean total IgE level of 499.7 ± 388.7 IU/mL, consistent with T2-high asthma. Patients reported an average of 2.3 ± 1.2 asthma exacerbations in the 6 months prior to treatment initiation. Most were on triple inhaler therapy (ICS/LABA/LAMA: 86.7%), with a smaller proportion on ICS/LABA (13.3%). The mean daily oral corticosteroid dose was 7.7 ± 4.6 mg of prednisolone or its equivalent.

Clinical Outcomes with Benralizumab Treatment

1. Asthma Control Test scores

Significant improvements in ACT scores were observed with benralizumab treatment over time. Patients experienced a mean increase in ACT scores from baseline to 6 months (5.88 ± 1.49, $p = 0.01$) and continued improvement at 12 months (5.57 ± 1.74, $p = 0.04$) (Fig. 2A). These results indicate enhanced asthma symptom control with benralizumab.

2. FEV1

Changes in lung function, as measured by FEV1, were statistically significant during benralizumab treatment. The mean FEV1 increase was 0.33 ± 0.11 L from baseline to 6 months ($p = 0.049$) and 0.056 ± 0.01 L from baseline to 12 months ($p = 0.010$), indicating statistically significant gains at both time points (Fig. 2B). These findings suggest measurable and sustained improvements in lung function with benralizumab treatment over 12 months.

3. Acute exacerbation of asthma

A substantial reduction in the frequency of AEs was achieved with benralizumab treatment. Patients experienced a mean decrease in exacerbations from baseline to 6 months (1.93 ± 0.35, $p = 0.0002$), as well as a reduction observed at 12 months (1.27 ± 0.29, $p = 0.0024$) (Fig. 2C). These results demonstrate the sustained efficacy of benralizumab in reducing asthma exacerbations throughout the 12-month treatment period.

4. Maintenance oral corticosteroid dose

Reductions in maintenance OCS use were both significant and sustained with benralizumab. The mean reduction in OCS dose was 4.53 ± 0.89 mg ($p = 0.0003$) from baseline to 6 months, with a sustained reduction of 5.00 ± 1.30 mg ($p = 0.006$) observed at 12 months (Fig. 2D). These findings highlight the potential of benralizumab to reduce systemic corticosteroid dependence in patients with severe asthma while maintaining effective disease control.

Changes in Type 2 Inflammatory Markers with Benralizumab Treatment

1. Blood eosinophil counts

A significant reduction in blood eosinophil counts was observed with benralizumab treatment. The mean decrease from baseline to 6 months was 435.2 ± 131.9 cells/μL ($p = 0.0151$), with a sustained reduction of 444.9 ± 128.9 cells/μL ($p = 0.0117$) at 12 months (Fig. 3A). These findings underscore the efficacy of benralizumab in depleting eosinophils and aligning with its targeted mechanism of action in manag-

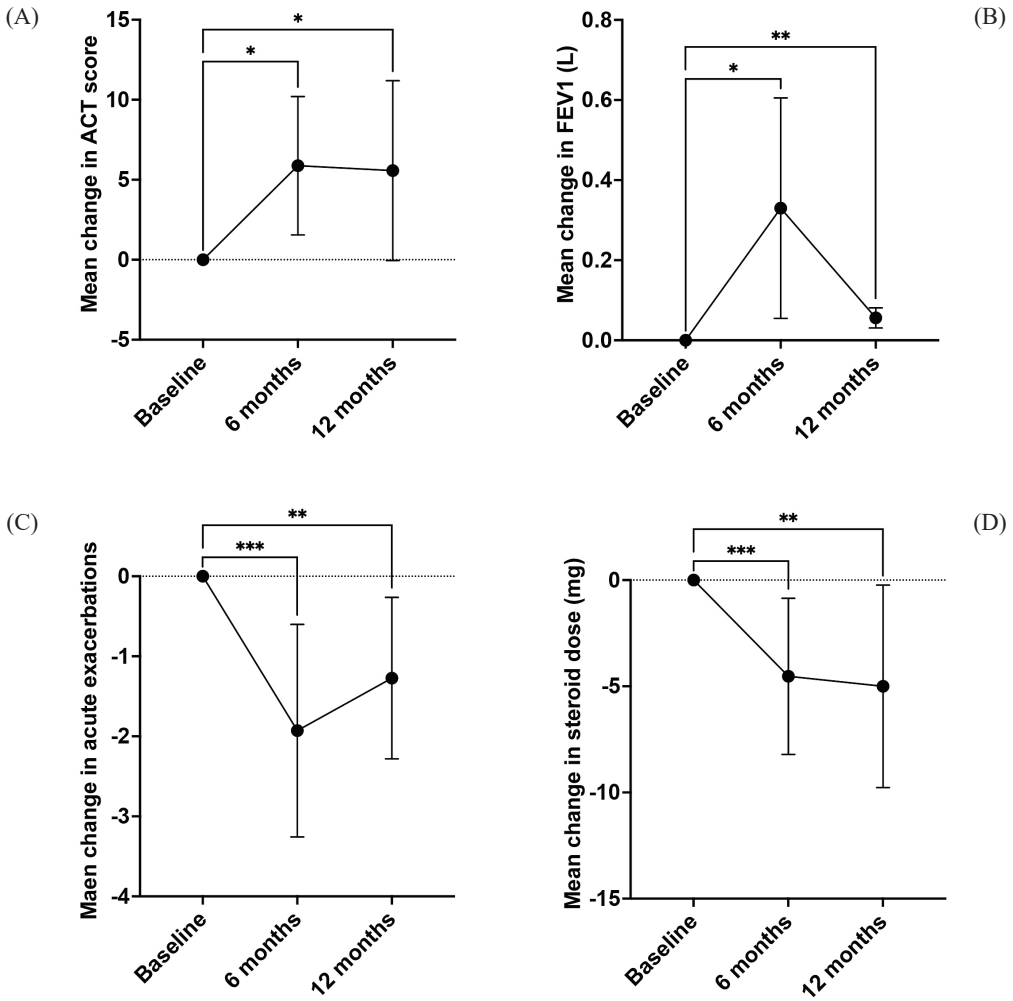

Fig. 2. Changes in clinical outcomes and treatment parameters over 12 months in patients with T2-high severe asthma treated with benralizumab. (A) Mean changes in Asthma Control Test (ACT) scores at baseline, 6 months, and 12 months. (B) Mean changes in forced expiratory volume in 1 second (FEV1, L) over the same time points. (C) Mean changes in the frequency of acute exacerbations. (D) Mean changes in oral corticosteroid dose (mg). Statistical significance is indicated as $*p < 0.05$, $**p < 0.01$, $***p < 0.001$. Error bars represent standard deviations.

ing severe eosinophilic asthma.

2. Total IgE levels

No significant changes in total IgE levels were detected during benralizumab treatment. The mean difference in total IgE levels from baseline to 6 months was -706.6 ± 372.8 KU/L ($p = 0.3069$), and from baseline to 12 months was 8.714 ± 305.2 KU/L ($p = 0.9995$) (Fig. 3B). These findings suggest that benralizumab has minimal impact on total IgE levels in patients with severe eosinophilic asthma.

Correlation Between Blood Eosinophil Counts and Total IgE Levels

A moderate positive correlation was observed between baseline blood eosinophil counts and baseline total IgE levels in patients treated with benralizumab, with a correlation coefficient of $r = 0.45$ ($p = 0.041$) (Fig. 3C).

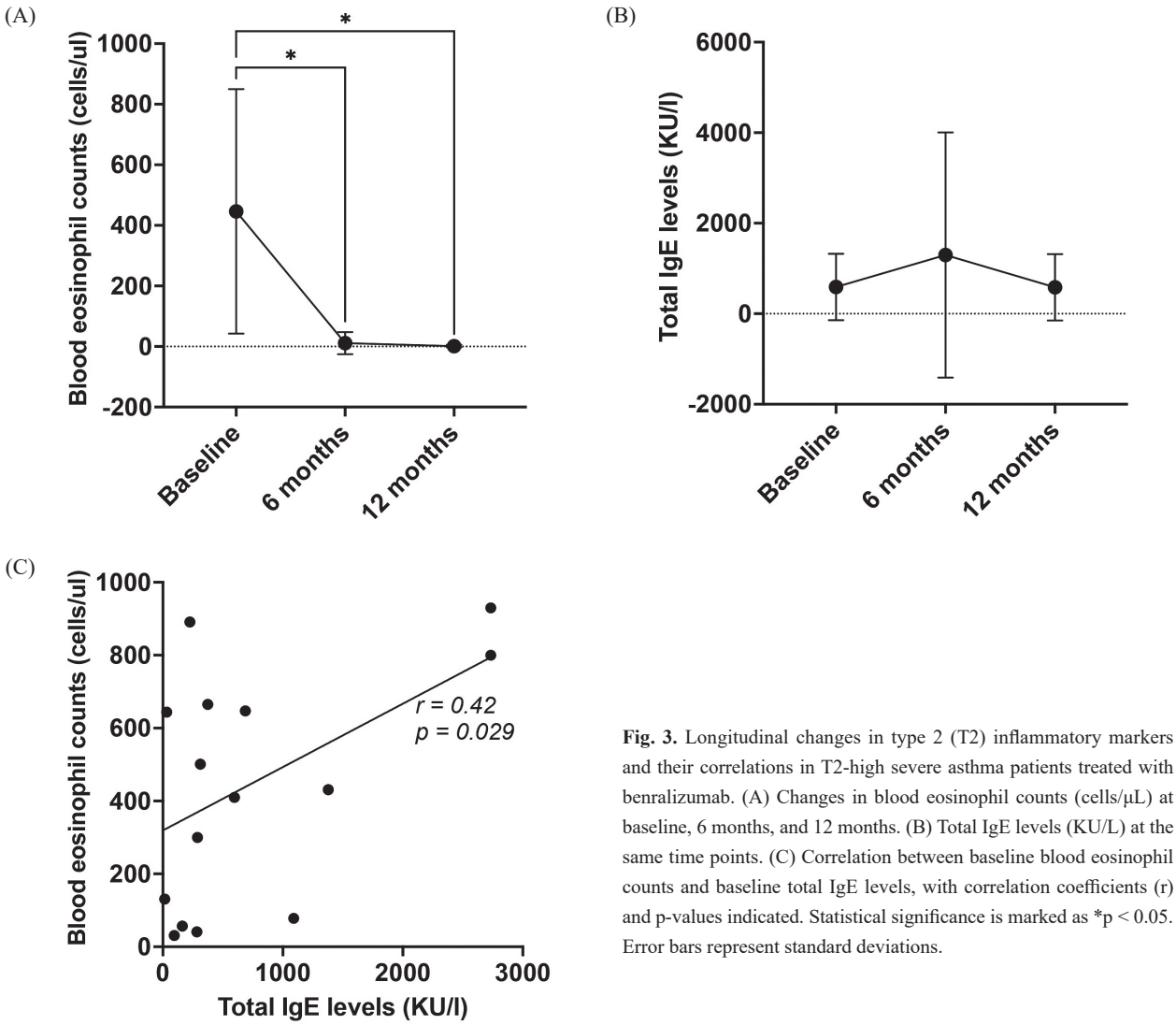

Fig. 3. Longitudinal changes in type 2 (T2) inflammatory markers and their correlations in T2-high severe asthma patients treated with benralizumab. (A) Changes in blood eosinophil counts (cells/μL) at baseline, 6 months, and 12 months. (B) Total IgE levels (KU/L) at the same time points. (C) Correlation between baseline blood eosinophil counts and baseline total IgE levels, with correlation coefficients (r) and p-values indicated. Statistical significance is marked as *p < 0.05. Error bars represent standard deviations.

These findings emphasize the relationship between T2 inflammatory markers and provide valuable insights into the immunological mechanisms underlying severe asthma.

Relationship Between Changes in Type 2 Inflammatory Markers and Clinical Outcome Improvements

The correlation heatmap revealed varying relationships between changes in T2 inflammatory markers (blood eosinophils and total IgE levels) and clinical outcome improvements during benralizumab treatment across different time points (Fig. 4). At baseline, blood eosinophil levels showed weak to moderate correlations with several clinical outcomes, though most did not reach statistical significance. Furthermore, blood eosinophil changes at 6 months showed a moderate inverse correlation with steroid use (r = -0.491, p = 0.063) and a weak correlation with AE reductions (r = 0.386, p = 0.155), though these were not statistically

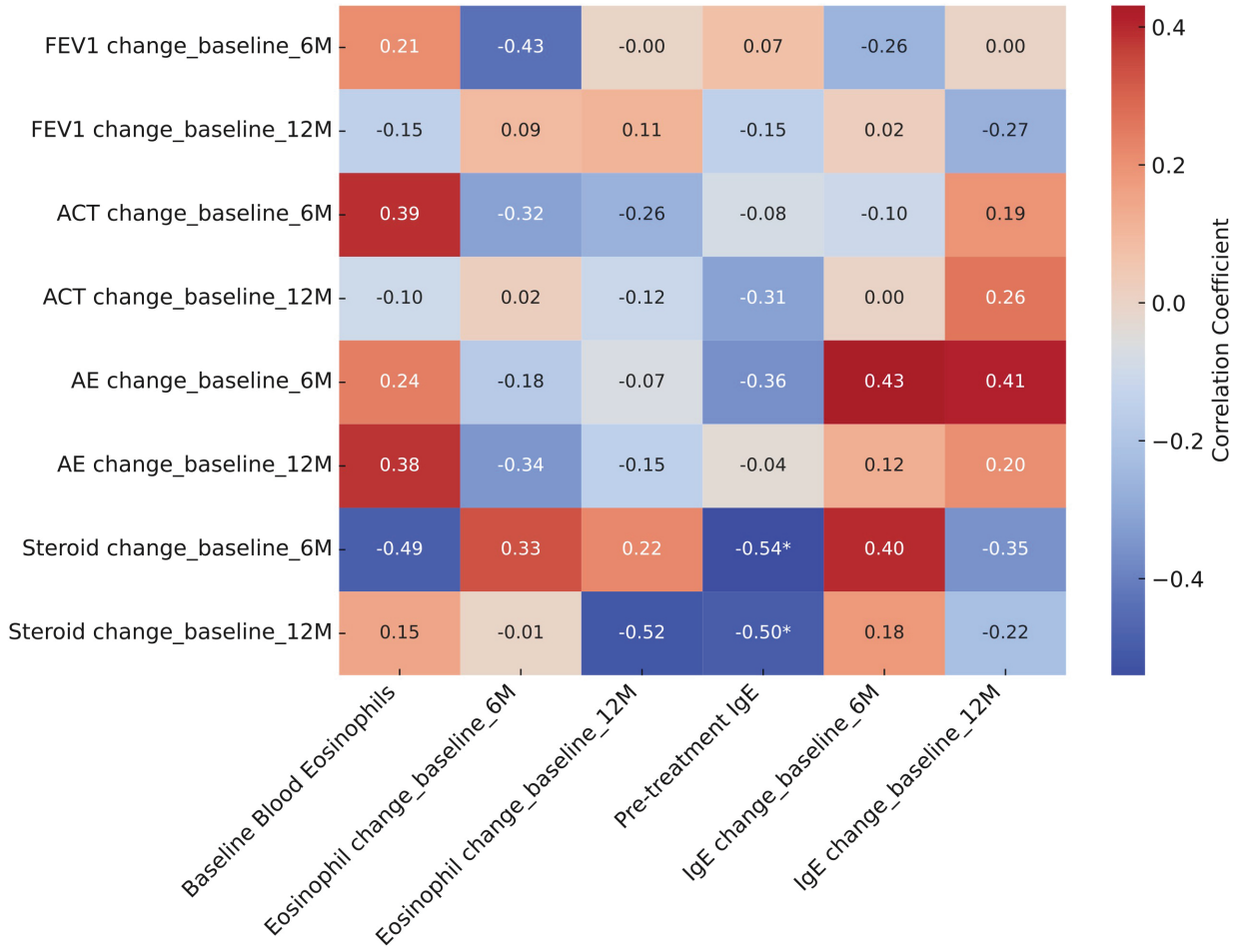

Fig. 4. Correlation heatmaps showing relationships between type 2 (T2) inflammatory markers (blood eosinophils and total IgE levels) and clinical outcomes (FEV1, ACT scores, exacerbation frequency, and steroid dose) in T2-high severe asthma patients treated with benralizumab. Positive correlations are red, and negative are blue, with intensity indicating strength. Significant correlations are marked as $*p < 0.05$. Data include baseline blood eosinophil counts, and changes in blood eosinophils and total IgE levels at 6 and 12 months.

significant. Similarly, blood eosinophil level changes at 12 months showed weaker associations with steroid use (r = -0.343, $p = 0.211$) and AE ($r = 0.333$, $p = 0.159$). These results, though not statistically significant, suggest a potential trend toward reduced systemic corticosteroid use and AE frequency associated with eosinophil depletion, warranting further investigation. Interestingly, baseline IgE levels showed a significant inverse correlation with reductions in steroid use at both 6 months ($r = -0.540$, $p = 0.038$) and 12 months ($r = -0.500$, $p = 0.049$), indicating that patients with higher baseline IgE levels might experience more substantial steroid-sparing effects. However, total IgE level changes over time did not demonstrate significant associations with any clinical outcomes, reflecting the limited impact of benralizumab on IgE dynamics. These findings highlight the distinct and multifaceted relationships between T2 biomarkers and clinical outcomes, underscoring the need for further investigation into

the predictive value of baseline markers and their role in guiding personalized asthma treatment strategies.

Discussion

This longitudinal study found that benralizumab significantly improves asthma control and lung function, reduces exacerbation rates, and decreases maintenance OCS use at both 6 and 12 months in patients with T2-high severe asthma. In addition, benralizumab had differential effects on T2 markers, markedly reducing blood eosinophil counts while having no significant impact on serum total IgE levels at these time points. Baseline blood eosinophil counts were moderately correlated with baseline serum total IgE levels. Notably, baseline total IgE levels were significantly associated with reductions in OCS use at 6 and 12 months during benralizumab treatment.

Benralizumab effectively depletes blood eosinophils to near-complete levels within 6 months, with this reduction consistently sustained over 12 months, as demonstrated both by previous clinical trials [11-12] and real-world evidence [13-15]. This reduction aligns with the drug's targeted mechanism of action, which is enhanced by targeting eosinophils through the IL-5 receptor α, with its afucosylated design increasing affinity for natural killer cells [16]. The dramatic eosinophil depletion led to significant and sustained improvements in ACT scores, exacerbation frequency, FEV1, and OCS reliance, with benefits achieved within 6 months and maintained over 12 months. These outcomes reflect the importance of eosinophil suppression in achieving disease control in T2-high asthma, consistent with findings from previous studies [11-12, 17-18].

Interestingly, despite its robust effect on eosinophils, benralizumab showed minimal impact on serum total IgE levels, which remained largely unchanged throughout the study period. This is consistent with research suggesting that anti-IL-5 therapies primarily target eosinophilic inflammation rather than IgE-driven pathways [12]. Our results are consistent with previous studies showing that benralizumab's clinical efficacy in reducing exacerbations and improving lung function is independent of total IgE levels [19-20]. Similarly, an observational study reported that while benralizumab effectively improve asthma outcomes, including steroid reduction, these benefits not associated with IgE levels, but appeared to be more pronounced in atopic patients [21]. In contrast, a retrospective cohort study reported a significant reduction in IgE levels with benralizumab, which was associated with improved asthma control and basophil depletion [22]. These findings suggest that IgE modulation may not be a primary mechanism of benralizumab's therapeutic effects, and instead, point to its role in eosinophil depletion as a key driver of clinical benefits.

The correlation between dynamic T2 markers, such as blood eosinophils and total IgE levels, and clinical outcomes in severe asthma remains complex and varies across studies. In our study, baseline blood eosinophil levels revealed weak to moderate correlations with several clinical outcomes, although these did not reach statistical significance. Similarly, correlations between changes in blood eosinophil levels and clinical outcomes, such as reductions in steroid use and exacerbation frequency, were moderate to weak, and also not statistically significant, suggesting that additional factors may contribute to these improvements. While we observed no significant changes in total IgE levels dur-

ing benralizumab treatment, baseline total IgE levels showed a significant inverse association with OCS reduction, indicating a potential predictive role for IgE. This differs from the findings of a previous study, which reported a reduction in IgE levels with benralizumab, along with associations with improved asthma control and basophil depletion [22]. These discrepancies underscore the variability in T2 marker dynamics across different patient populations and study methodologies. Further research is warranted to elucidate the underlying mechanisms of biomarker-specific effects contributing to OCS reduction during benralizumab treatment.

The strengths of this study lie in its evaluation of the longitudinal effects of benralizumab on dynamic changes in T2 biomarkers and improvements across various clinical outcomes over a 12-month period, providing valuable insights into its impact in patients with T2-high severe asthma. The inclusion of multiple outcome measures, such as ACT scores, FEV1, exacerbation frequency, and OCS use, allows for a holistic assessment of treatment efficacy. In addition, the correlation analysis between baseline and dynamic changes in biomarkers with clinical outcomes offers a detailed understanding of the potential predictive value of T2 markers. However, this study has several limitations. The relatively small sample size may have limited the statistical power to detect some correlations. Furthermore, the study cohort consisted exclusively of patients treated at a single center, which may affect the generalizability of the findings to broader populations. While the study evaluated biomarkers at 3 time points, the long-term effects of benralizumab beyond 12 months were not assessed. Finally, as the study focused on eosinophilic severe asthma, the findings may not fully apply to patients with mixed or non-eosinophilic phenotypes, highlighting the need for further research in diverse asthma subgroups.

Conclusion

Benralizumab demonstrates substantial efficacy in improving asthma control, reducing exacerbations, and minimizing OCS use in patients with T2-high severe asthma. While no significant changes in total IgE levels were observed, baseline total IgE levels correlated with OCS reduction at 6 months and 12 months, suggesting a complex interaction between T2 biomarkers and outcomes. These findings support the use of benralizumab as an effective treatment for T2-high severe asthma and emphasize the need for further research into biomarker-driven personalized strategies.

Acknowledgments

We would like to thank Miss Hsiao-Huang Chuang for her assistance in applying for biological therapies through the National Health Insurance (NHI) program.

References

1. (GINA), G.I.f.A. Global Strategy for Asthma Management and Prevention. 2024, Global Initiative for Asthma.
2. Fahy JV. Type 2 inflammation in asthma--present in most, absent in many. Nat Rev Immunol 2015; 15(1): 57-65.
3. Brusselle GG, Koppelman GH. Biologic therapies for severe asthma. N Engl J Med 2022; 386(2): 157-171.
4. Shah PA, Brightling C. Biologics for severe asthma--Which, when and why? Respirology 2023; 28(8): 709-721.
5. Sridhar S, Liu H, Pham T-H, *et al*. Modulation of blood inflammatory markers by benralizumab in patients with

eosinophilic airway diseases. Respir Res 2019; 20(1): 14.
6. Menzies-Gow A, Hoyte FL, Price DB, *et al*. Clinical remission in severe asthma: a pooled post hoc analysis of the patient journey with benralizumab. Adv Ther 2022; 39(5): 2065-2084.
7. Farne HA, Wilson A, Milan S, *et al*. Anti-IL-5 therapies for asthma. Cochrane Database Syst Rev 2022; 7(7): CD010834.
8. FitzGerald JM, Bleeker ER, Menzies-Gow A, *et al*. Predictors of enhanced response with benralizumab for patients with severe asthma: pooled analysis of the SIROCCO and CALIMA studies. Lancet Respir Med 2018; 6(1): 51-64.
9. Quanjer PH, Stanojevic S, Cole JT, *et al*. Multi-ethnic reference values for spirometry for the 3-95-yr age range: the global lung function 2012 equations. Eur Respir J 2012; 40(6): 1324-43.
10. Standardization of Spirometry, 1994 Update. American Thoracic Society. Am J Respir Crit Care Med 1995; 152(3): 1107-36.
11. Bleecker ER, FitzGerald JM, Chanez P, *et al*. Efficacy and safety of benralizumab for patients with severe asthma uncontrolled with high-dosage inhaled corticosteroids and long-acting beta(2)-agonists (SIROCCO): a randomised, multicentre, placebo-controlled phase 3 trial. Lancet 2016; 388(10056): 2115-2127.
12. FitzGerald JM, Bleeker ER, Parameswaran N, *et al*. Benralizumab, an anti-interleukin-5 receptor alpha monoclonal antibody, as add-on treatment for patients with severe, uncontrolled, eosinophilic asthma (CALIMA): a randomised, double-blind, placebo-controlled phase 3 trial. Lancet 2016; 388(10056): 2128-2141.
13. Ghassemian A, Park JJ, Tsoulis MW, *et al*. Targeting the IL-5 pathway in eosinophilic asthma: a comparison of mepolizumab to benralizumab in the reduction of peripheral eosinophil counts. Allergy Asthma Clin Immunol 2021; 17(1): 3.
14. Numata T, Miyagawa H, Nishioka S, *et al*. Efficacy of benralizumab for patients with severe eosinophilic asthma: a retrospective, real-life study. BMC Pulm Med 2020; 20(1): 207.
15. Pelaia C, Crimi C, Benfante A, *et al*. Therapeutic effects of benralizumab assessed in patients with severe eosinophilic asthma: real-life evaluation correlated with allergic and non-allergic phenotype expression. J Asthma Allergy 2021; 14: 163-173.
16. Dagher R, Kumar V, Copenhaver AM, *et al*. Novel mechanisms of action contributing to benralizumab's potent anti-eosinophilic activity. Eur Respir J 2022; 59(3).
17. Canonica GW, Consani L, Malerba L, *et al*. Effects of benralizumab in patients with severe eosinophilic asthma (SEA): a plain language summary of the ANANKE study. Immunotherapy 2024; 16(14-15): 913-923.
18. Pini L, Bagnasco D, Beghe B, *et al*. Unlocking the long-term effectiveness of benralizumab in severe eosinophilic asthma: a three-year real-life study. J Clin Med 2024; 13(10).
19. Chipps BE, Newbold P, Hirsch I, *et al*. Benralizumab efficacy by atopy status and serum immunoglobulin E for patients with severe, uncontrolled asthma. Ann Allergy Asthma Immunol 2018; 120(5): 504-511 e4.
20. Jackson DJ, Humbert M, Hirsch I, *et al*. Ability of serum IgE concentration to predict exacerbation risk and benralizumab efficacy for patients with severe eosinophilic asthma. Adv Ther 2020; 37(2): 718-729.
21. Sposato B, Ricci A, Camiciottoli G, *et al*. Influence of allergic status and nasal polyposis on long-term Benralizumab response in eosinophilic severe asthma. Clin Ter 2023; 174(1): 67-74.
22. Contoli M, Santus P, Menzella F, *et al*. Effects of anti-IL5 biological treatments on blood IgE levels in severe asthmatic patients: a real-life multicentre study (BIONIGE). Clin Transl Allergy 2022; 12(4): e12143.

Graves' Disease Complicated with Left Subclavian Vein Thrombosis and Subsequent Chylothorax: A Unique Case Report

Hung-Teng Yen[1], Meng-Rui Lee[1], Ching-Yi Lee[2], Shih-Wei Lee[2], Kuan-Yu Chen[1]

A 52-year-old man with a history of irregularly controlled hyperthyroidism presented with exertional dyspnea, left upper limb swelling, and rapid weight loss. Diagnostic imaging revealed a diffusely enlarged goiter, right lower lung pulmonary embolism, left subclavian vein thrombosis, bilateral massive pleural effusion, and massive ascites. Graves' disease was diagnosed based on compatible symptoms, signs, elevated free thyroxine, suppressed thyroid-stimulating hormone, and positive thyrotropin-binding inhibitor immunoglobulin. The patient was then treated with carbimazole. Diagnostic thoracentesis, and paracentesis revealed chylothorax and chylous ascites. Lymphangiography showed slowed passage of lymph, abnormal reflux of lymph into the mediastinum, and a dilated thoracic duct that ended at the thrombosed segment of left subclavian vein. Despite interventions including thoracentesis, nil per os status, total parenteral nutrition, and anticoagulation therapy, the patient showed limited improvement, necessitating advanced interventions such as thrombectomy and catheter-directed thrombolysis. Follow-up showed a decreasing trend in pleural effusion, and the patient was then discharged smoothly. This case highlights a rare presentation of Graves' disease with subsequent left subclavian vein thrombosis, complicated by bilateral chylothorax and chylous ascites, not previously reported in the literature. ***(Thorac Med 2026; 41: 77-83)***

Key words: Chylothorax, deep vein thrombosis, left subclavian vein thrombosis, Graves' disease, hyperthyroidism

Introduction

Chylothorax, defined as a pleural effusion containing chyle [1], is relatively uncommon and accounts for around 3% of all pleural effusions [2]. The mechanism of chylothorax includes direct trauma to the thoracic duct, obstruction of the thoracic duct, and transdiaphragmatic chyle movement. It is mostly caused by trauma and malignancies, which are responsible for 50% and 30% of cases, respectively [3]. Central venous thrombosis is an uncommon

[1]Chest Division, Internal Medicine Department, National Taiwan University Hospital, 2Chest Division, Internal Medicine Department, Taoyuan General Hospital.
Address reprint requests to: Dr. Hung-Teng Yen, No. 7, Zhongshan S Road, Zhongzheng District, Taipei City, Taiwan.

cause of chylothorax, usually developed after central venous catheterization [3]. Thromboembolism is a rare complication of Graves' disease [4]. Here, we present a case featuring these 3 rare conditions.

Case Presentation

A 52-year-old man with a history of hyperthyroidism presented to the emergency department of a local hospital with a 3-day history of exertional dyspnea. He reported being in his usual state of health until approximately 2 years prior, when he developed neck swelling, palpitations, and significant weight loss (from 80 kg to 70 kg over 3 months). He was diagnosed with hyperthyroidism and treated with thiamazole and propranolol for 4 months, but discontinued follow-up due to a desire to lose more weight. His weight further decreased to 50 kg 2 months before admission, prompting a return to medical care and resumption of propranolol and methimazole, although adherence was poor.

He reported chronic productive cough with whitish sputum for 2 years, occasionally yellowish or blood-tinged in appearance. He was a heavy smoker (2 packs/day for ~40 years) and worked at a breakfast shop. There was no known tuberculosis contact. His family history was notable for an aunt who died of colon cancer.

Three days before admission, he developed exertional dyspnea—no symptoms on level ground, but breathlessness when climbing stairs. Chest radiograph at a local clinic revealed left-side pleural effusion, and he was referred to a local hospital. On arrival, vital signs showed tachycardia (125 bpm) and elevated blood pressure (143/76 mmHg). Physical examination revealed decreased breath sounds over bilateral lower lung fields, WHO grade 2 goiter, exophthalmos, and non-pitting edema of the left arm (noted by the patient for 2 months). No lower limb edema or adventitious lung sounds were observed.

Laboratory data revealed neutrophil-predominant leukocytosis (14,870/μL, segmented neutrophils 88.4%), elevated C-reactive protein (5.9 mg/dL), elevated N-terminal pro b-type natriuretic peptide (2299.4 pg/mL), elevated d-dimer (16.79 mg/L), elevated free T4 (2.17 ng/dL), and low thyroid-stimulating hormone (TSH) (<0.008 μIU/mL). Albumin was low (2.9 g/dL), and sodium mildly decreased (131 mmol/L).

Chest + abdomen + pelvis computed tomography (CT) showed a diffusely enlarged thyroid, right lower lung pulmonary embolism, left subclavian vein thrombosis, bilateral massive pleural effusion, and massive ascites. Left thoracentesis was performed, with 1000 ml of yellow-orange and turbid pleural effusion drained (Fig. 1). The pleural effusion analysis

Fig. 1. Gross appearance of the patient's left pleural effusion. The fluid was milky in nature, with coloration ranging from yellow-orange to pinkish, consistent with chylous effusion.

showed transudate using Light's criteria. Paracentesis yielded 900 ml of light-yellow and turbid ascites, with a serum-ascites albumin gradient of 0.9 g/dL. Both fluids had elevated triglyceride levels, indicating chylothorax and chylous ascites.

Although his dyspnea improved after initial thoracentesis, his pleural effusion reaccumulated rapidly. He was placed on nil per os status and started on total parenteral nutrition to reduce chyle production. Enoxaparin was initiated and later switched to edoxaban for thromboembolism. Methimazole 20 mg/day was used for hyperthyroidism.

After a month of treatment, there was little improvement in chylothorax and left arm swelling. The patient was referred to our hospital for further evaluation and management.

At our facility, repeated thoracentesis with bilateral pigtail catheter insertion again confirmed chylous effusions (Table 1). Lab data showed persistent hyperthyroidism, and Graves' disease was later confirmed by the presence of TSH receptor antibodies (Table 2). Tumor markers, autoimmune profiles, and some inherited thrombophilia work-up were then done (Table 3). Chest + abdomen + pelvis CT (Fig. 2) and a whole-body positron emission to-

Table 1. Lab data for Llft Pleural Effusion

Pleural effusion routine								Cytology
Total nucleated cell (TNC) (/μL)	RBC count (/μL)	Neutrophil (%)	Mesothelial cell & histiocyte (%)	Lymphocyte (%)	Eosinophil (%)			No malignancy
2913	11000	11	14	75	0			
Biochemistry								
Total protein (g/dL)	LDH (U/L)	Glucose (mg/dL)	Triglyceride (mg/dL)	Total cholesterol (mg/dL)	Amylase (U/L)	Lipase (U/L)	Adenosine deaminase (ADA) (U/L)	
<3	165	129	805	60	24	62	4	
Microbiology								
Gram's stain			Aerobic pathogen	Anaerobic pathogen	Fungus	Acid fast stain	Mycobacterium culture	TB PCR
PMN (/LPF)	Mononuclear (/LPF)	No bacteria	Negative	Negative	Negative	Negative	Negative	Negative
1-9	>25							

Note: Right pleural effusion and ascites were checked and had similar results.

Table 2. Thyroid Functions and Thyroid Autoantibodies

Free T4 (ng/dL)	hsTSH (μIU/mL)	T3 (ng/dL)	Anti-TPO Ab (AMA) (IU/mL)	Anti- thyroglobulin Ab (TA) (IU/ML)	% inhibition of TSH binding
1.4	<0.0038	530.6	>2000	138.78	94.5

Table 3. Other Etiology Surveys for a Hypercoagulable State

Tumor markers			**Other**		
CEA (ng/mL)	SCC (ng/mL)	CA 19-9 (U/mL)	Vitamin B12 (pg/mL)	Folic acid (ng/mL)	Homocysteine (μmol/L)
1.19	1.0	15.5	192	2.8	12.95

APS profile					
DRVVT	Anti-β2 GP1 (U/mL)	IgM anticardiolipin (MPL)	IgG anticardiolipin (GPL-U/mL)	IgM antiphospholipid Ab (MPL)	IgG antiphospholipid Ab (GPL)
Not detected	1.3	5.04	1.1	5.57	0.21

Other autoimmune profiles						
C3 (mg/dL)	C4 (mg/dL)	ANA	Anti-dsDNA (WHO units/mL)	Anti ribosomal P (U/mL)	Anti-ENA	electrophoresis
130.86	39.35	1:160+ (AC-8, AC-19)	13.32	1.0 (Negative)	0.09 (Negative)	Polyclonal gammopathy

Anti-coagulation function				
Antithrombin III function	Protein C function	Protein S function	Plasminogen function	α2 antiplasmin
98.1%	96.5%	102.5%	92.8%	31.7%

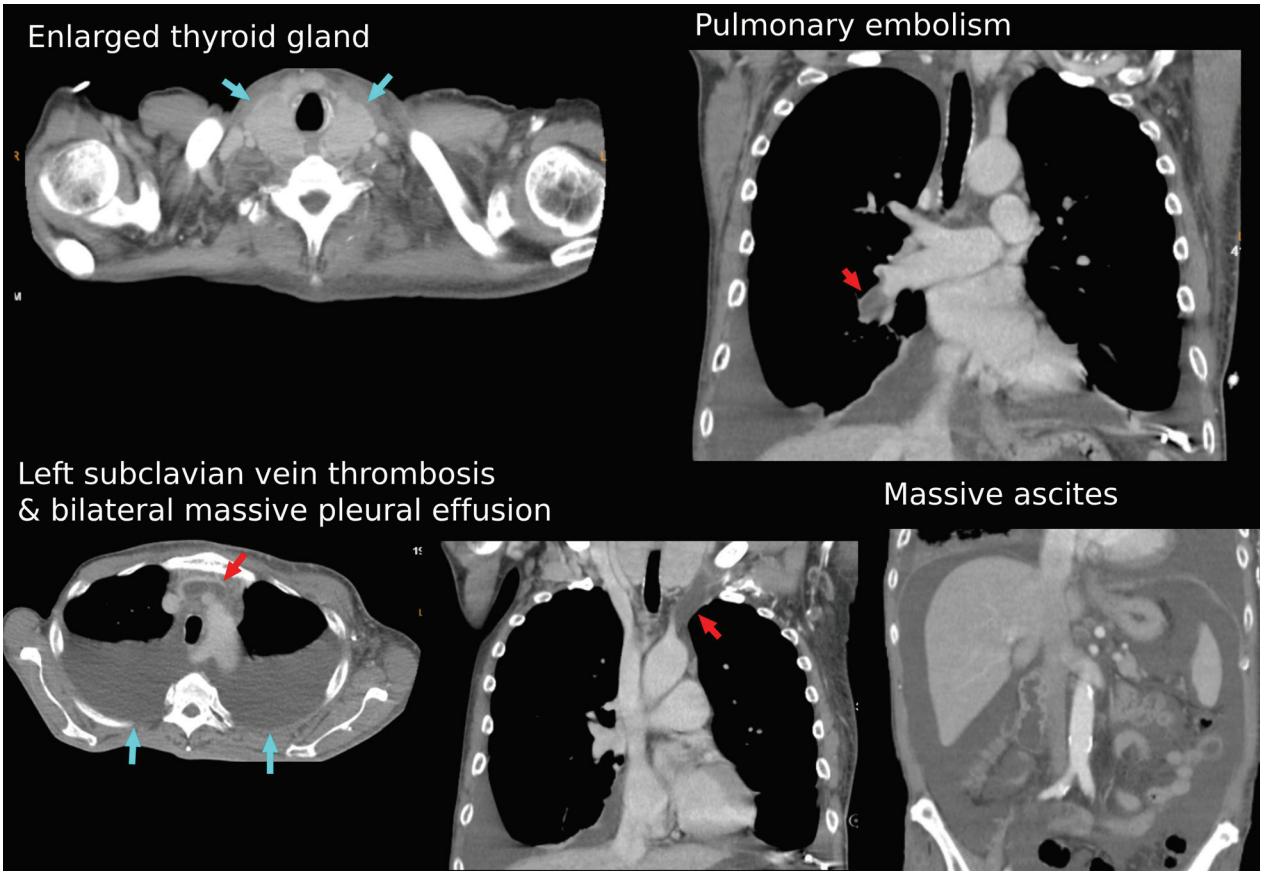

Fig. 2. Contrast-enhanced computed tomography (CT) scan of the chest, abdomen, and pelvis.

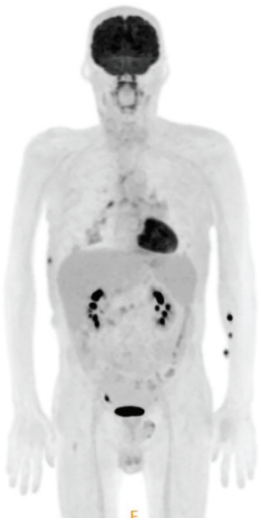

Fig. 3. Whole-body positron emission tomography (PET) scan. The scan revealed inflammatory changes in bilateral atelectatic lungs and mild hypermetabolic activity in the pulmonary hilar and mediastinal lymph nodes, suggesting lymphadenitis. No evidence of malignancy was observed.

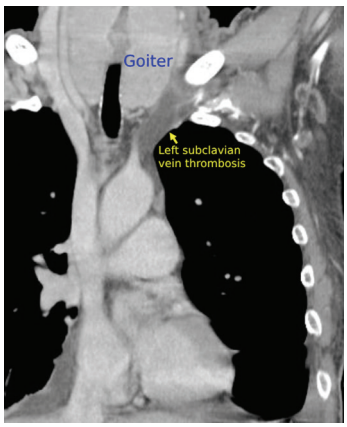

Fig. 4. Coronal CT image of the left thoracic inlet. No direct compression of the left subclavian vein by the enlarged thyroid (goiter) was identified.

mography scan (Fig. 3) were performed to rule out malignancy and to follow up the burden of thromboembolism. The CT still showed only a slight decrease in the burden of thrombus compared to the previous CT image. Although the goiter was adjacent to the left subclavian vein, it didn't compress the vein (Fig. 4). Lymphangiography (Fig. 5) showed slowed passage of

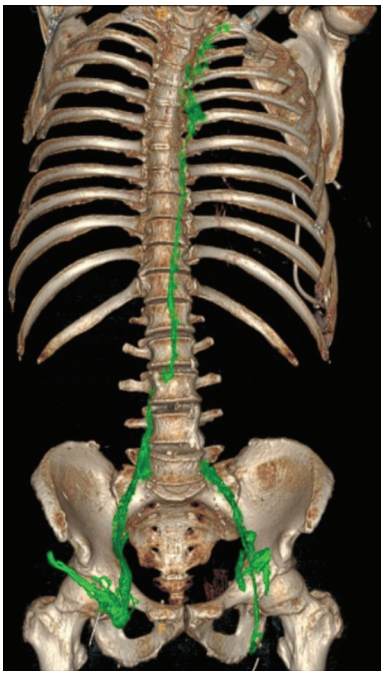

Fig. 5. Lymphangiography. Abnormal lymphatic reflux into the mediastinum was observed, along with a dilated thoracic duct terminating at the thrombosed segment of the left subclavian vein.

lymph, abnormal reflux of lymph into the mediastinum, and a dilated thoracic duct that ended at the thrombosed segment of the left subclavian vein.

The patient received full-dose enoxaparin (60 mg Q12H), followed by catheter-directed thrombolysis, thrombectomy, and stenting of the left subclavian vein due to limited response to anticoagulation alone. Post-intervention drainage showed a decreasing trend in the pleural effusion. The patient was discharged in stable condition with plans for outpatient follow-up.

Discussion

We reported a rather rare cause of thoracic duct obstruction -- left subclavian vein thrombosis.

Although chyle typically contains a protein concentration within the transudative range (2–3 g/dL), chylothorax is mostly exudate [5]. The elevated protein content observed in most chylothoraces is thought to result from the physiologic reabsorption of water and small solutes across capillary membranes under normal transcapillary hydrostatic gradients [5].

Transudative chylothorax is an uncommon entity, with limited etiologies including nephrotic syndrome, hepatic cirrhosis, heart failure, amyloidosis, and superior vena cava obstruction [6, 7]. In our patient, the pleural fluid protein level was less than 3 g/dL, suggesting a transudative profile. This finding served as an early clue that the chylothorax may have been secondary to central venous thrombosis.

Lymphangiography showing a dilated thoracic duct that ended at the thrombosed left subclavian vein was direct proof of the thrombus causing thoracic duct obstruction. Left subclavian vein thrombosis causing chylothorax has been reported multiple times [8-15]. The most common etiology of these cases of thrombosis is the placement of a central venous catheter, and the most common population with this complication is infants.

Though Graves' disease has been reported to lead to a hypercoagulable state, it is an uncommon complication [16]. Graves' disease has been reported to cause chylothorax by direct oppression of the thoracic duct by a goiter [17-18], but it has never been reported to cause central venous thrombosis. The most common thromboembolism site following thyrotoxicosis is cerebral venous thrombosis [19-22]. An increased risk of pulmonary embolism was also found among patients with hyperthyroidism [23]. Many pathophysiologic mechanisms behind Graves' disease and thromboembolism have been proposed, but they have not been confirmed [4]. One study suggested a potential association between thyrotoxicosis and hyperhomocysteinemia resulting from vitamin B deficiency and subsequent thromboembolic events [24]. Therefore, we also checked out the patient's vitamin B levels. He did have mild folic acid deficiency, but his homocysteine level was normal. As central venous thrombosis following Graves' disease has not been reported before, we also searched for other causes of a hypercoagulable state, but no other risk factor was identified.

Conclusion

This case highlights a rare presentation of Graves' disease with subsequent left subclavian vein thrombosis, complicated by bilateral chylothorax and chylous ascites, not previously reported in the literature.

References

1. McGrath EE, Blades Z, and Anderson PB. Chylothorax: aetiology, diagnosis and therapeutic options. Respir Med 2010; 104(1): 1-8.
2. Bhatnagar M., Fisher A, Ramsaroop S, *et al*. Chylothorax: pathophysiology, diagnosis, and management-a comprehensive review. J Thorac Dis 2024; 16(2): 1645-1661.
3. Skouras V, Kalomenidis I. Chylothorax: diagnostic approach. Curr Opin Pulm Med 2010; 16(4): 387-93.
4. Ordookhani A, Burman KD. Hemostasis in overt and subclinical hyperthyroidism. Int J Endocrinol Metab 2017; 15(3): e44157.
5. Agrawal V, Doelken P, Sahn SA. Pleural fluid analysis in chylous pleural effusion. Chest 2008; 133(6): 1436-1441.
6. Diaz-Guzman E, Culver DA, Stoller JK. Transudative chylothorax: report of two cases and review of the literature. Lung 2005; 183(3): 169-75.
7. Bhardwaj H, Bhardwaj B, Awab A. Transudative

chylothorax in a patient with liver cirrhosis: a rare association. Heart Lung 2015; 44(4): 363-5.
8. Kramer SS, Taylor GA, Garfinkel DJ, *et al*. Lethal chylothoraces due to superior vena caval thrombosis in infants. AJR Am J Roentgenol 1981; 137(3): 559-63.
9. Seibert JJ, Golladay ES, Keller C, Chylothorax secondary to superior vena caval obstruction. Pediatr Radiol 1982; 12(5): 252-4.
10. Dhande V, Kattwinkel J, Alford B. Recurrent bilateral pleural effusions secondary to superior vena cava obstruction as a complication of central venous catheterization. Pediatrics 1983; 72(1): 109-13.
11. Van Veldhuizen PJ, Taylor S. Chylothorax: a complication of a left subclavian vein thrombosis. Am J Clin Oncol 1996; 19(2): 99-101.
12. Manghat N, Hancock J, Walsh M, *et al*. Thrombolysis for central venous occlusion causing bilateral chylothorax in a patient with Down syndrome. J Vasc Interv Radiol 2004; 15(5): 511-5.
13. Husain SJ, Sadiq F, Zubairi AB, *et al*. Massive unilateral chylous pleural effusion: a rare initial presentation of Behcet's disease. Singapore Med J 2006; 47(11): 978-80.
14. Berkenbosch JW, Monteleone PM, Tobias JD. Chylothorax following apparently spontaneous central venous thrombosis in a patient with septic shock. Pediatr Pulmonol 2003; 35(3): 230-3.
15. Ünal M, Ünal E, Imholz ALT. Chylothorax due to thrombosis of the jugular and subclavian veins in a patient with gastric cancer: a case report. J Med Case Rep 2023; 17(1): 75.
16. Franchini M, Lippi G, Targher G. Hyperthyroidism and venous thrombosis: a casual or causal association? A systematic literature review. Clin Appl Thromb Hemost 2011; 17(4): 387-92.
17. Hiroi N, Sakamoto Y, Urita Y, *et al*. Graves' disease with intractable diarrhea, chylous ascites, and chylothorax: a case report. Thyroid 2007; 17(12): 1299-303.
18. Young Oh S, Kim BH, Kim DY, *et al*. Chylothorax associated with substernal goiter in Graves' disease treated with radioactive iodine. Int J Endocrinol Metab 2017; 15(2): e41787.
19. Verberne HJ, Fliers E, Prummel MF, *et al*. Thyrotoxicosis as a predisposing factor for cerebral venous thrombosis. Thyroid 2000; 10(7): 607-10.
20. Siegert CE, Smelt AH, de Bruin TW. Superior sagittal sinus thrombosis and thyrotoxicosis. Possible association in two cases. Stroke 1995; 26(3): 496-7.
21. Ra CS, Lui CC, Liang CL, *et al*. Superior sagittal sinus thrombosis induced by thyrotoxicosis. Case report. J Neurosurg 2001; 94(1): 130-2.
22. Mouton S, Nighoghossian N, Berruyer M, *et al*. Hyperthyroidism and cerebral venous thrombosis. Eur Neurol 2005; 54(2): 78-80.
23. Lin HC, Yang LY, Kang JH. Increased risk of pulmonary embolism among patients with hyperthyroidism: a 5-year follow-up study. J Thromb Haemost 2010; 8(10): 2176-81.
24. Colleran KM, Ratliff DM, Burge MR. Potential association of thyrotoxicosis with vitamin B and folate deficiencies, resulting in risk for hyperhomocysteinemia and subsequent thromboembolic events. Endocr Pract 2003; 9(4): 290-5.

Giant Bulla Appearing Like Tension Pneumothorax: A Case Report

Sheng-Fu Chen[1], Yi-Ching Yang[2], Te-Chun Shen[1,3]

Giant bullae are large air-filled spaces in the lungs that can mimic tension pneumothorax in both symptoms and imaging, posing a diagnostic challenge. A 24-year-old male presented with progressive dyspnea. Chest radiography revealed hyperlucency and mediastinal shift. Computed tomography (CT) confirmed a giant bulla in the right lung. Surgical bullectomy was performed, and the patient recovered well postoperatively. Giant bullae can resemble tension pneumothorax radiographically and clinically. CT imaging is essential for accurate diagnosis. Misdiagnosis may lead to inappropriate interventions such as chest tube insertion, causing serious complications. Clinical awareness is critical to avoiding iatrogenic harm. ***(Thorac Med 2026; 41: 84-87)***

Key words: giant bulla; pneumothorax; computed tomography (CT)

Introduction

Giant bullae are large, air-filled spaces in the lung, often resulting from chronic smoking-related alveolar destruction [1]. They can compress surrounding lung tissue and cause respiratory symptoms. Radiographically, giant bullae may closely resemble tension pneumothorax, especially on chest X-rays, making differentiation challenging [2]. Accurate diagnosis is essential to prevent inappropriate interventions such as chest tube insertion, which may lead to complications. Here, we present the case of a young man with a giant bulla mimicking tension pneumothorax.

Case Presentation

A 24-year-old young male without a specific medical history or congenital disorders, except for a 10-year habit of smoking half a pack of cigarettes daily, presented with progressive shortness of breath over the past 6 months. The patient denied any fever, body weight loss,

[1]Division of Pulmonary and Critical Care Medicine, Department of Internal Medicine, China Medical University Hospital, China Medical University, Taichung, Taiwan. [2]Department of Education, China Medical University Hospital, China Medical University, Taichung, Taiwan. [3]Division of Critical Care Medicine, Chu Shang Show Chwan Hospital, Nantou, Taiwan.
Address reprint requests to: Dr. Te-Chun Shen, Division of Pulmonary and Critical Care Medicine, Department of Internal Medicine, China Medical University Hospital, China Medical University, No. 2, Yu-De Road, Taichung 404, Taiwan.

cough, sputum production, chest pain, or chest tightness. Physical examination revealed an increased respiratory rate (22/min) and decreased tactile fremitus, hyperresonance on percussion, and diminished breathing sounds on the right side. No wheezing was heard. Chest radiography (Fig. 1) showed an enlarged right lung with displacement of the heart and significantly reduced lung markings on the right side, but no visible pleural line. A computed tomography (CT) scan (Fig. 2) confirmed the presence of a giant bulla. Due to the significant size of the bulla and the resulting respiratory symptoms, the patient consented to surgical treatment (Fig. 3). Postoperative follow-up showed good recovery with relief of the compression (Fig. 4).

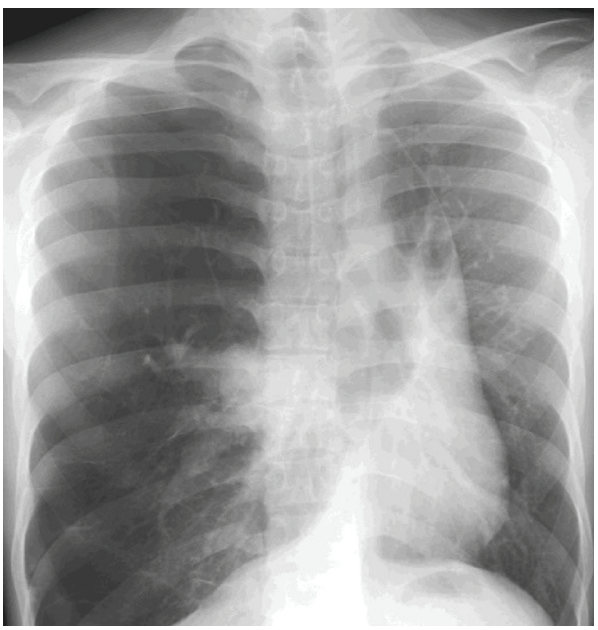

Fig. 1. Chest radiography showed an enlarged right lung and reduced lung markings.

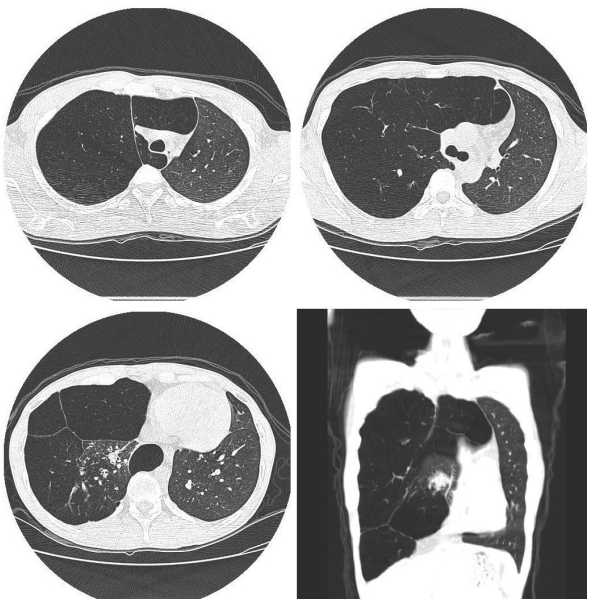

Fig. 2. Computed tomography confirmed the presence of a giant bulla.

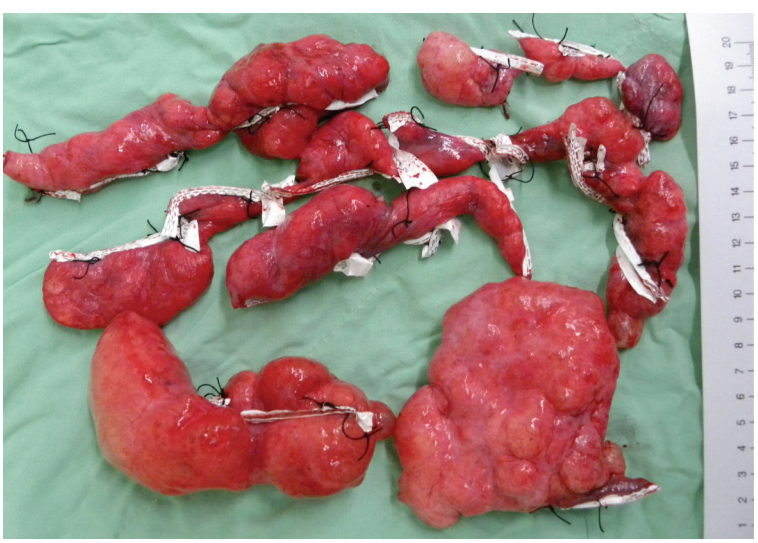

Fig. 3. Severe diffuse emphysematous changes were noted at the RUL and RML. Partial resection was performed smoothly.

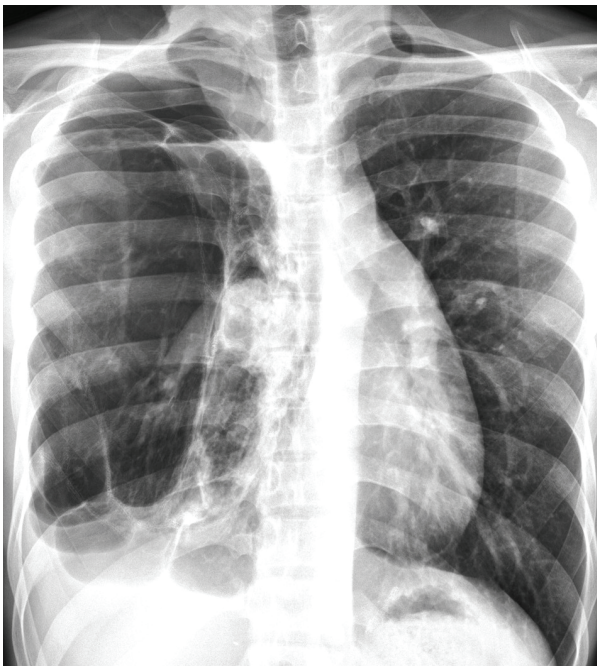

Fig. 4. Chest radiography at the 2-month follow-up showed relief of the compression.

Discussion

Giant bullae are large air-filled spaces within the lung, usually defined as occupying more than 30% of a hemithorax [1]. They commonly develop as a result of chronic alveolar wall destruction due to smoking-related emphysema. However, other contributing factors include marijuana smoking, intravenous drug use, and connective tissue disorders such as Marfan syndrome. In some cases, giant bullae may also occur idiopathically, particularly in younger patients without a significant smoking history [3-5]. The mechanism involves progressive coalescence of adjacent emphysematous spaces, which lose their structural support and expand, leading to compression of adjacent functional lung parenchyma. Over time, this can result in respiratory compromise, exertional dyspnea, and even symptoms mimicking a mass effect [3-5].

One of the major clinical challenges is distinguishing a giant bulla from a tension pneumothorax, as both conditions can present with acute dyspnea, chest hyperlucency on imaging, diminished breathing sounds, and mediastinal shift. On chest radiographs, giant bullae typically appear as radiolucent areas with thin or imperceptible walls, often located in the upper lobes. They may be confused with pneumothorax, especially when the pleural line is not clearly visible. A key radiographic distinction lies in the shape of the pleural interface: in pneumothorax, the pleural line is usually convex toward the chest wall, while in giant bullae, the line—if visible—is often concave [2].

The definitive imaging modality for differentiation is CT, which provides detailed cross-sectional anatomy, showing the precise location, size, and borders of the bullae, and confirming whether air is located within lung tissue (bullae) or in the pleural space (pneumothorax). The "double-wall sign," where air outlines both sides of a bulla wall, may help distinguish giant bullae from true pneumothorax; however, it can be misleading when adjacent bullae mimic pleural air [2]. Thus, comprehensive evaluation of multiple CT slices is essential.

The consequences of misdiagnosing a giant bulla as a tension pneumothorax can be serious. Inappropriate insertion of a chest tube into a bulla can cause complications such as bleeding, infection, persistent air leak, or even worsening of respiratory distress. Several cases have illustrated that unnecessary thoracic drainage failed to relieve symptoms, while surgery or conservative oxygen therapy provided clinical improvement once the correct diagnosis was made [3-5].

Conclusion

Giant bullae form through progressive alveolar destruction and expansion, and can closely mimic tension pneumothorax on imaging and clinical presentation. Accurate differentiation—especially using CT—is essential to guide proper management and avoid iatrogenic complications. Awareness of the subtle imaging distinctions and clinical context is critical in preventing harmful interventions in patients with bullous lung disease.

References

1. Huang W, Han R, Li L, *et al*. Surgery for giant emphysematous bullae: case report and a short literature review. J Thorac Dis 2014; 6: E104-107.
2. Aramini B, Ruggiero C, Stefani A, *et al*. Giant bulla or pneumothorax: how to distinguish. Int J Surg Case Rep 2019; 62: 21-23.
3. Schumann M, Hamed A, Kohl T. Giant bulla imitating tension pneumothorax. Dtsch Arztebl Int 2019; 116: 461.
4. Chang CH, Ko HJ. Giant bulla or pneumothorax. Postgrad Med J 2022; 98: e51.
5. Ye Y, Zhan Y. Giant pulmonary bullae mistaken for pneumothorax. Am J Emerg Med 2024; 83: 162-162.

Intraoperative Nerve Monitoring-Assisted Tracheal Resection for Post-Intubation Tracheal Stenosis: A Case Report

Ying-Shian Chen[1,2], Yi-Hsiang Lai[3], Tsai-Wang Huang[3]

Tracheal resection for post-intubation tracheal stenosis (PITS) poses significant risks, particularly to the recurrent laryngeal nerves (RLN), due to dense fibrosis and proximity to the larynx. Intraoperative nerve monitoring (IONM), although widely adopted in thyroid surgery, is rarely used in tracheal surgery due to challenges in airway access and electrode positioning. We reported the case of a 73-year-old man with PITS successfully managed with tracheal resection and bilateral RLN monitoring using IONM. Customized intraoperative strategies allowed for safe nerve identification despite limited space and difficult anatomy. The patient recovered without hoarseness or vocal cord palsy, suggesting that IONM may offer functional benefits in selected high-risk tracheal surgeries. ***(Thorac Med 2026; 41: 88-94)***

Key words: intraoperative nerve monitoring, tracheal resection, recurrent laryngeal nerve

Introduction

Post-intubation tracheal stenosis (PITS) is an uncommon but potentially debilitating condition, with an estimated annual incidence of 0.049%. Tracheal resection and reconstruction remain rare, and complex procedures typically are performed in specialized centers. Benign tracheal conditions such as PITS pose distinct challenges due to fibrosis, adhesions, and altered anatomy, particularly in patients with prior tracheostomy or multiple airway interventions. This report describes a case of cricotracheal resection utilizing intraoperative nerve monitoring (IONM), highlighting its potential benefits in preserving recurrent laryngeal nerve function during high-risk surgery.

Case Presentation

The patient was a 73-year-old male with a history of chronic obstructive pulmonary disease (COPD) and coronary artery disease, who underwent coronary artery bypass grafting in October 2024. Approximately 2 months postoperatively, he presented to the emergency

[1]Surgery, Taichung Armed Forces General Hospital, Taichung 41168, Taiwan. [2]School of Medicine, National Defense Medical University, Taipei, Taiwan11490, Taiwan. [3]Surgery, Tri-Service General Hospital, National Defense Medical University, Taipei City 11490, Taiwan
Address reprint requests to: Dr. Tsai-Wang Huang, Surgery, Tri-Service General Hospital, National Defense Medical University, No. 325, Sec. 2, Chenggong Rd., Neihu District, Taipei City 11490, Taiwan.

department with exertional dyspnea and audible stridor. Initial evaluation excluded heart failure, and an acute exacerbation of COPD was suspected based on clinical presentation. He received oxygen therapy, bronchodilators, corticosteroids, and antibiotics, resulting in partial symptom improvement. However, persistent expiratory stridor raised concern about central airway obstruction.

Chest computed tomography (CT) revealed suspected tracheal stenosis at the T1 vertebral level. Bronchoscopy confirmed a lesion 5 cm below the vocal cords, with approximately 70% luminal narrowing—consistent with grade II stenosis based on the Myer-Cotton classification.

Initial airway management included an open tracheostomy performed on January 30, 2025, at the level of the first tracheal ring, using Blue Rhino dilatation and placement of an 8-mm Bivona tracheostomy tube. The tube was exchanged for a Teflon tracheostomy tube on February 4, 2025, due to ongoing secretion management issues. Despite this, the patient continued to experience exertional dyspnea, and suctioning became ineffective as the catheter could not be advanced.

On February 15, emergency bedside intubation with a 5-mm endotracheal tube was performed due to increasing airway obstruction. A follow-up bronchoscopy on February 21 showed worsening stenosis, now beginning 3 cm below the vocal cords with approximately 50% narrowing. On February 24, the patient underwent balloon dilatation via rigid bronchoscopy, followed by successful extubation and transfer to the general ward.

Given persistent airway narrowing and the failure of conservative and endoscopic interventions, the patient was referred to our institution for definitive surgical management.

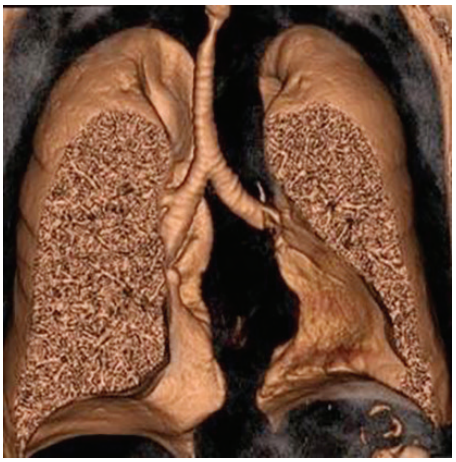

Fig. 1. Preoperative 3D reconstruction image showing upper tracheal stenosis.

Preoperative Assessment

Repeat chest CT after balloon dilatation and 3D reconstruction confirmed the presence of a high-grade upper tracheal stenosis (Fig. 1).

Anesthesia and Surgical Procedure

General anesthesia was induced using propofol (3 mcg/mL target-controlled infusion), fentanyl (1 mL), remimazolam (5 mg), and adjunctive agents per protocol. Due to anticipated airway difficulty from high-grade tracheal stenosis, the patient underwent awake nasal fiberoptic intubation using an Ambu® aScope™ 4 Broncho (Regular 5.0/2.2; 180°/180°). After visual confirmation of tracheal passage, a 6-mm endotracheal tube was successfully advanced beyond the vocal cords. Once airway control was secured, rocuronium (Esmeron) 50 mg was administered to facilitate muscle relaxation.

IONM was performed using the NIM 3.0 Response Monitoring System (Medtronic Xomed, Jacksonville, FL, USA), with proper electrode positioning confirmed by Glidescope-

assisted visualization of vocal cord function prior to incision.

A low transverse collar incision was made at the neck. The strap muscles were divided along the midline and retracted laterally. The thyroid isthmus was divided to expose the trachea. IONM facilitated identification and preservation of both recurrent laryngeal nerves (RLNs), with stronger signal amplitude noted on the left (Fig. 2). The stenotic segment, including 2 affected tracheal rings, was carefully mobilized and resected (Fig. 3A), with an estimated resection length of 2.5 cm. The upper resection margin was approximately 0.5 cm inferior to the cricoid cartilage.

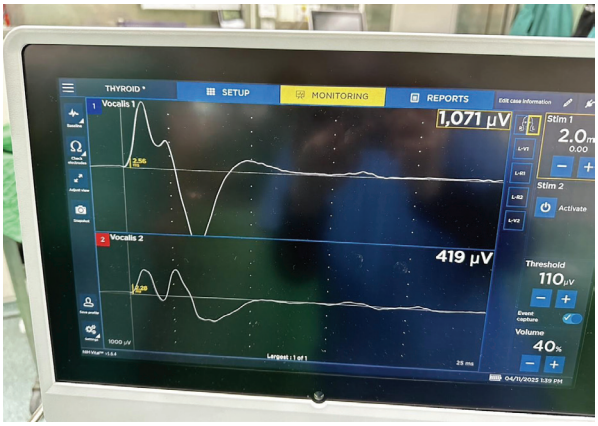

Fig. 2. Strong signal from the RLN detected on the IONM monitor.

After transection, the oral endotracheal tube was withdrawn proximally, and a sterile tube was inserted into the distal tracheal stump to maintain ventilation. Interrupted sutures, including the anterior row, were pre-placed. The proximal tube was then passed through the

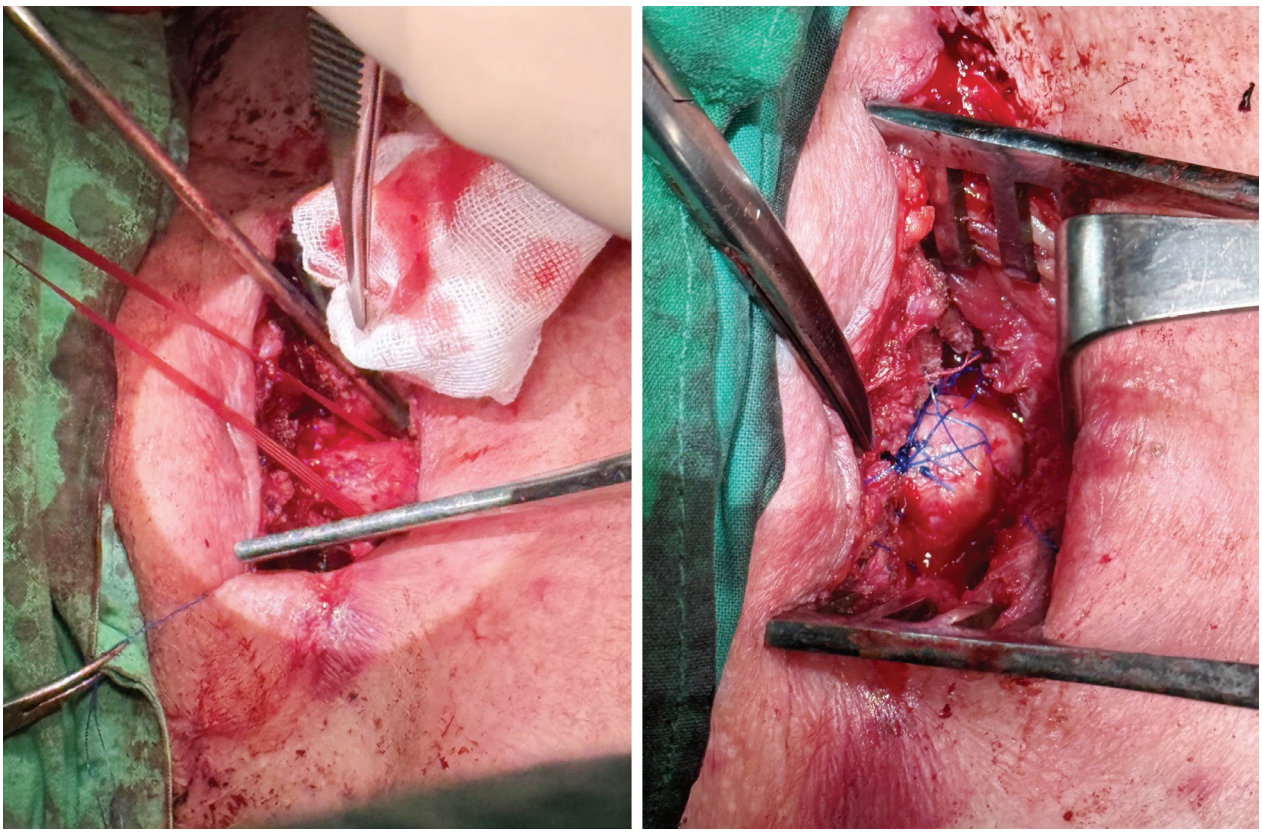

Fig. 3. Intraoperative view of the trachea. A. Exposure of the stenotic segment. B. Completion of cricotracheal anastomosis following resection of the stenotic tracheal rings.

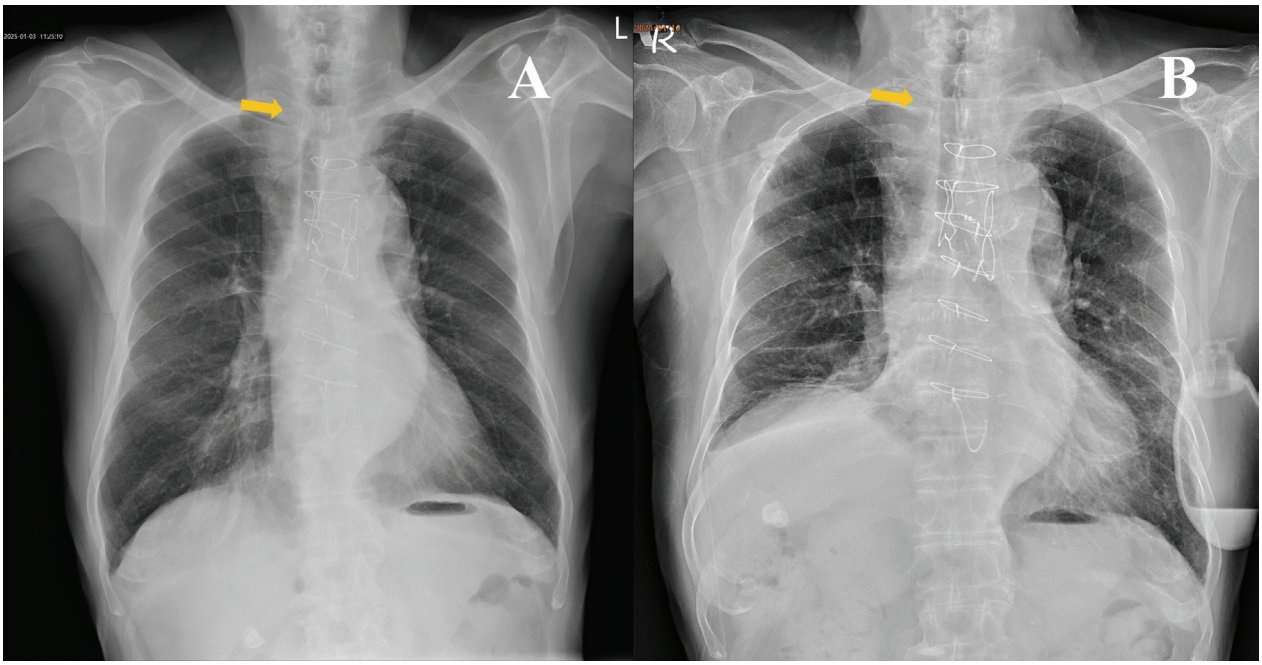

Fig. 4. A. Preoperative and B. postoperative chest radiographs revealing improved tracheal patency following cricotracheal resection.

anastomotic site under direct vision, ensuring no entanglement with the sutures. The sutures were tied sequentially under even tension (Fig. 3B). A submersion test revealed no air leak. To minimize tension at the anastomotic site, a guardian chin-to-sternum suture (Ethibond) was placed to maintain neck flexion postoperatively.

Intraoperative blood loss was minimal. The patient was transferred to the surgical intensive care unit in stable condition. He was extubated successfully on postoperative day 1, showing smooth respiratory function and no hoarseness. He was transferred to the general ward on postoperative day 3.

On postoperative day 6, the patient inadvertently hyperflexed his neck, leading to dislodgement of the guardian suture. Mild subcutaneous emphysema and air leakage through the Jackson-Pratt (JP) drain were noted. Conservative management was implemented, and the air leak resolved by postoperative day 10. The JP drain was subsequently removed, and the patient was discharged in stable condition on postoperative day 12. Preoperative and postoperative chest radiographs (Fig. 4A and 4B) illustrate the anatomical improvement following cricotracheal resection.

Discussion

Post-intubation tracheal stenosis (PITS) is a rare condition, with an incidence of 0.049% annually [1-2]. Tracheal resection and reconstruction remain relatively uncommon procedures, often centralized to high-expertise centers due to the complexity and rarity of the operation [3]. This case highlights the application of IONM in a cricotracheal resection complicated by prior tracheostomy and distorted anatomy—an uncommon scenario with limited precedent in existing literature. Compared with resections for malignancy, tracheal resection for benign

conditions such as PITS presents greater surgical challenges due to extensive fibrosis, altered tissue planes, and peritracheal adhesions caused by chronic inflammation or previous procedures like tracheostomy and interventions such as endoscopic dilation, laser therapy, cryotherapy, or stenting [4]. These factors distort normal anatomy, complicate dissection, and elevate the risk of injury to adjacent structures, particularly the RLN.

Although the incidence of permanent RLN palsy in tracheal surgery is relatively low (3.1–8.2%) in high-volume centers [5-6], even temporary injury can significantly affect postoperative phonation and airway protection. IONM, widely adopted in thyroid surgery [7], has been proposed as a method to reduce RLN injury during tracheal resections. However, to date, only 1 study has specifically addressed the use of IONM in this context. A retrospective review by Kadakia *et al*. over a 10-year period evaluated the use of IONM during tracheal resections across a mixed cohort of benign and malignant cases with variable degrees of stenosis. The study concluded that while IONM was feasible, it did not significantly reduce the incidence of nerve injury [5].

According to Brunete and colleagues, IONM may be particularly useful in 2 clinical scenarios: revision surgeries and upper cricotracheal resections [8]. In revision surgeries, the RLN is often embedded in scar tissue, making identification and preservation difficult, especially after a prior thyroid isthmectomy. In upper cricotracheal resections, lateral dissection may expose or even transect the RLN if not performed with caution.

In our case, while formal revision surgery had not been performed, a prior tracheostomy had resulted in significant peritracheal fibrosis and anatomical distortion—features commonly encountered in revision settings. Furthermore, the resection involved the upper trachea adjacent to the cricoid cartilage, aligning with Brunet's proposed indications for IONM. This anatomical complexity justified the use of intraoperative nerve monitoring, even though it was not a classic revision case.

Despite its potential, IONM faces technical limitations. In-field distal tracheal intubation is often required, which may displace electrodes away from the vocal cords. In cases of critical stenosis, the IONM tube may not be compatible due to size constraints. Additional challenges include managing analgesia and the presence of previous tracheostomy sites [9].

Intraoperative localization of the stenosis was complicated by poor visibility. Although simultaneous bronchoscopy or needle puncture could have aided localization, performing these maneuvers was technically difficult with the IONM tube in place. Optimizing the tube position for nerve monitoring conflicted with visualization and access for precise marking, highlighting the trade-off between nerve preservation and resection accuracy.

In our case, several customized intraoperative strategies were employed to address these limitations. Preoperative chest CT and bronchoscopy were used to estimate the stenotic segment's location—approximately 3 cm below the vocal cords and 2 cm from the sternal notch—providing critical external reference points. Intraoperatively, after dividing the thyroid isthmus and exposing the fibrotic and adherent trachea, careful lateral dissection was performed under IONM guidance to avoid injury to the RLNs. Once the fibrotic adhesions were cleared, the affected tracheal segment became externally visible. To ensure safety, we

first made an incision in the mid-portion of the visibly stenotic segment, and then, under direct vision, further trimmed the trachea to achieve appropriate proximal and distal margins while preserving adjacent structures.

At this point, the IONM endotracheal tube was withdrawn proximally, and a new standard endotracheal tube was inserted into the distal trachea to maintain ventilation. This exchange allowed for a clear surgical field and secure airway management.

To prepare for possible intubation difficulties, preemptive rigid bronchoscopy was planned for dilation if necessary. Additionally, if the stenosis could not be clearly identified externally, a 5-mm bronchoscope was available as a backup for intraoperative localization. However, this approach would require the anesthesiology team to remain on standby due to the risks associated with tube withdrawal and the need to reconfirm optimal electrode positioning to maintain effective nerve monitoring.

This case, the first tracheal resection performed in our department, may offer practical insight into the role of IONM in complex airway surgery. While current evidence on IONM's protective effect remains inconclusive, it proved to be a valuable intraoperative tool in our experience. IONM not only confirmed nerve integrity, but also guided careful dissection through dense fibrotic tissue. Even an experienced surgical team benefited from real-time neuromonitoring in this high-risk scenario.

Innovative approaches, such as direct insertion of electrodes into the endolaryngeal muscles via the thyroid cartilage, have been described to address some of IONM's limitations [10]. Although available studies do not yet report statistically significant reductions in RLN injury with IONM, its value lies in the real-time functional assessment of nerve integrity, which facilitates immediate surgical adjustments and supports intraoperative decision-making.

In this patient, vocal cord function appeared intact based on clinical observation, although no objective laryngoscopic evaluation was performed. This represents a limitation. While this case supports the feasibility of IONM in complex airway surgery, its generalizability may be limited by institutional resources and procedural expertise. The patient remained clinically stable during outpatient follow-up. A chest CT scan was scheduled for 3 months postoperatively to assess any restenosis or anastomotic complications. To date, only 2 original studies have described IONM use in tracheal surgery, and further research is warranted to define its role in different clinical contexts [5, 8].

Conclusion

This case underscores the potential value of IONM in complex airway surgery. While not universally adopted, IONM provided real-time feedback that aided safe dissection and nerve preservation in a challenging case of post-intubation tracheal stenosis. Further studies are needed to better define the indications and benefits of IONM in tracheal procedures.

References

1. Nouraei SAR, Ma E, Patel A, *et al*. Estimating the population incidence of adult post-intubation laryngotracheal stenosis. Clin Otolaryngol 2007; 32: 411-12.
2. Nordin U. The trachea and cuff-induced tracheal injury. An experimental study on causative factors and prevention. Acta Otolaryngol Suppl 1977; 345: 1-71.
3. Stanifer BP, Andrei AC, Liu M, *et al*. Short-term outcomes of tracheal resection in the Society of Thoracic

Surgeons Database. Ann Thorac Surg 2018; 106: 1612-18.
4. Brichet A, Verkindre C, Dupont J, *et al*. Multidisciplinary approach to management of postintubation tracheal stenoses. Eur Respir J 1999; 13: 888-93.
5. Kadakia S, Sinha P, Wiebe K, *et al*. The role of intraoperative nerve monitoring in tracheal surgery: 20-year experience with 110 cases. Pediatr Surg Int 2017; 33: 1091-96.
6. Piazza C, Del Bon F, Paderno A, *et al*. Complications after tracheal and cricotracheal resection and anastomosis for inflammatory and neoplastic stenoses. Ann Otol Rhinol Laryngol 2014; 123: 798-804.
7. Randolph GW, Dralle H, Abdullah H, *et al*. Electrophysiologic recurrent laryngeal nerve monitoring during thyroid and parathyroid surgery: International standards guideline statement. Laryngoscope 2011; 121 Suppl 1: S1-16.
8. Brunet A, Rovira A, Quer M, *et al*. Recurrent laryngeal nerve intraoperative neuromonitoring indications in non-thyroid and non-parathyroid surgery. J Clin Med 2024; 13: 2221.
9. Karapinar K, Kose EA. The anesthesia of trachea and bronchus surgery. Korean J Anesthesiol 2016; 69: 333-40.
10. Piazza C, Del Bon F, Paderno A, *et al*. Intraoperative nerve monitoring in laryngotracheal surgery. Cir Esp (Engl Ed) 2017; 95: 397-99.